Distinct transcriptional programs of SOX2 in different types of small cell lung cancers

Running title

Distinct role of SOX2 in lung cancer.

Authors

Yuki Tenjin[1, 2], Kumi Matsuura[3], Shinji Kudoh[1], Shingo Usuki[4], Tatsuya Yamada[1, 5], Akira Matsuo[1], Younosuke Sato[1], Haruki Saito[1, 6] , Kosuke Fujino[1, 5], Joeji Wakimoto[7], Takaya Ichimura[8], Hirotsugu Kohrogi[9], Takuro Sakagami[2], Hitoshi Niwa[3], Takaaki Ito[1]

Affiliations

Departments of [1] Pathology and Experimental Medicine, [2] Respiratory Medicine, [5] Thoracic Surgery, and [6] Otolaryngology-Head and Neck Surgery, Kumamoto University, Graduate School of Medical Science Kumamoto University, Graduate School of Medical Science, Honjo 1-1-1, Chuo-ku, Kumamoto 860-8556, Japan.

16 [3] Department of Pluripotent Stem Cell Biology, [4] Liaison Laboratory Research Promotion

17 Center (LILA), Institute of Molecular Embryology and Genetics, Kumamoto University,

18 Honjo 2-2-1, Chuo-ku, Kumamoto 860-0811, Japan.

19 [7] Division of Pathology, Minami Kyushu National Hospital, Kagoshima, 899-5293, Japan.

20 [8] Department of Pathology, Saitama Medical University Faculty of Medicine, Saitama

21 350-0495, Japan.

22 [9] Department of Respiratory Medicine, Omuta Tenryo Hospital, Tenryo 1-100, Omuta,

23 Fukuoka 836-8556, Japan.

24

Abstract

SOX2 is an oncogene in human small cell lung cancer (SCLC), an aggressive neuroendocrine (NE) tumor. However, the roles of SOX2 in SCLC remain unclear, and strategies to selectively target SOX2 in SCLC cells have not yet been established. We herein demonstrated that SOX2 is involved in NE differentiation and tumorigenesis in cooperation with ASCL1, a lineage-specific transcriptional factor, in the classical subtype of SCLC cell lines. ASCL1 recruits SOX2, which promotes INSM1 expression. Precursor SCLC lesions were established in *Trp53* (-/-); *CCSP*rtTA; tetO*Cre*; floxed*Rb1*; floxed*Hes1* mice, and the NE neoplasms induced were positive for Ascl1, Sox2, and Insm1. In contrast to the ASCL1-SOX2 signaling axis to control the SCLC phenotype in classical subtype SCLC, SOX2 targeted distinct genes, such as those related to the Hippo pathway, in ASCL1-negative, variant subtype SCLC. The present results support the importance of the ASCL1-SOX2 axis as a main subtype of SCLC, and suggest the therapeutic potential of targeting the ASCL1-SOX2 signaling axis and the clinical utility of SOX2 as a biological marker in the classical subtype of SCLC.

Keywords

ASCL1; classical subtype; variant subtype Small cell lung carcinoma; SOX2

Introduction

Lung cancer is the leading cause of cancer-related mortality worldwide. Small cell lung cancer (SCLC) accounts for approximately 14% of all lung cancers and is genetically considered to be one of the most aggressive malignant neuroendocrine (NE) tumors (Byers *et al.*, 2015). Despite high response rates to first-line treatment, SCLC cases show rapid growth and metastasis and acquire multidrug resistance. The median survival of patients with SCLC is 7 months, and this has not markedly changed in the last few decades (Wang *et al.*, 2017). The development of novel target molecules in therapies for SCLC remains limited. The findings of basic studies on the molecular mechanisms underlying small cell carcinogenesis have yet to be clarified, and advances in novel therapeutic development are expected (Gazdar *et al.*, 2017).

The World Health Organization (WHO) Classification recognizes SCLC as a relatively homogeneous tumor, with pure SCLC and combined SCLC subtypes (Travis *et al.,* 2015). Approximately 30 years ago, Gazdar *et al.* reported the different forms of the "classic" and "variant" subtypes of SCLC. Classical SCLC cells are characterized by floating cell growth and distinct NE differentiation, and variant SCLC cells by adhesive growth and poor NE differentiation (Gazdar *et al.,* 1985; Carney *et al.,* 1985). Classical cell lines belong to NE

high SCLC, which may be associated with the increased expression of Achaete-Scute complex homologue 1 (ASCL1), a member of the basic helix-loop-helix (bHLH) family of transcription factors. On the other hand, the variant cell lines belong to NE low SCLC, which is associated with the activation of *NOTCH*, *Hippo*, and *RE-1 silencing transcription factor* (*REST*) genes and prominent epithelial-to-mesenchymal (EMT) transition resulting in a mesenchymal phenotype (Lim JS *et al.,* 2017, Zhang *et al.,* 2018). ASCL1 was previously shown to be expressed at a high frequency in SCLC (Ball *et al.,* 1993). Furthermore, the knockdown of *ASCL1* induced growth inhibition and apoptosis in SCLC cell lines (Osada *et al.,* 2005, 2008). Insulinoma-associated protein 1 (INSM1) is a crucial regulator of NE differentiation in lung cancer, and is specifically expressed in SCLC, along with ASCL1 (Fujino *et al.,* 2015). Borromeo *et al.* (2016) reported that Ascl1 played a pivotal role in tumorigenesis in mouse models of SCLC, and also suggested that *SOX2* and *INSM1* were target genes of ASCL1. In human SCLC, *SOX2* was recognized as an oncogene because *SOX2* amplification was detected in some SCLCs, and *SOX2* gene suppression inhibited the cell proliferative capacity of SCLC cell lines (Rudin *et al.,* 2012).

The major aim of the present study is to elucidate the mechanisms by which SOX2 affects the phenotype and heterogeneity of SCLC. We hypothesized that SOX2 may contribute to distinct transcriptional programs and biological characteristics in both the

79 classical and variant subtypes of SCLC. To test this hypothesis, the present study was
80 designed to investigate the following: (1) a comparison of the target genes of SOX2 in human
81 SCLC cell lines by a chromatin immunoprecipitation sequence (ChIP-seq) analysis. (2) the
82 relationship between ASCL1 and SOX2 in SCLC cell lines, surgically-resected tissues, and
83 mouse SCLC precursor lesions, and (3) the functional difference in SOX2 between the
84 classical and variant subtypes of human SCLC cell lines. We herein demonstrated that
85 SOX2 was more strongly expressed in some SCLC than non-SCLC (NSCLC). SOX2
86 regulates distinct transcriptional programs in both the classical and variant subtypes of
87 SCLC, and, in the classical subtype, functions in an ASCL1-dependent manner.
88
89 **Results**
90 **SOX2 is overexpressed and targeted distinct genes between classical and variant subtypes**
91 **of SCLC cell lines**
92 To examine SOX2 expression patterns, we performed a Western blot (WB) analysis of
93 12 lung cancer cell lines (7 SCLCs, 3 adenocarcinomas (ADCs), and 2 squamous cell
94 carcinomas (SCCs)). The WB analysis revealed that the SOX2 protein was generally
95 expressed at markedly higher levels in all SCLC cell lines examined than in the NSCLC cell
96 lines. This result suggested that SOX2 plays a more pivotal role in SCLC cell lines. Four out

97 of the 7 SCLC cell lines simultaneously expressed SOX2, ASCL1, and INSM1 (Fig. 1A).
98 There are two subtypes of SCLC cell lines, classical and variant, which are distinguished by
99 their morphologies or NE properties. The loss of the expression of a master transcriptional
100 factor, such as ASCL1, is often associated with the properties of variant SCLC cell lines
101 (Zhang *et al.,* 2018). In the present study, H69, H889, SBC1, and H1688 belonged to the
102 classical subtype of SCLC cell lines, which were positive for ASCL1 and INSM1. In contrast,
103 H69AR, SBC3, and SBC5 were classified as the variant subtype of SCLC cell lines, which
104 were negative for ASCL1. We then conducted ChIP-seq to analyze SOX2 target genes in the
105 H69, H889, and SBC3 cell lines. We also combined the results of the RNA-seq analysis for
106 these cell lines, which showed the global expression levels of mRNAs. As shown in a Venn
107 plot, we identified 346 SOX2-bound genes (shared in NCI-H69 and NCI-H889) that were
108 specifically occupied in the classical subtypes and expressed at higher levels in the classical
109 subtypes than in the variant subtype (Fig. 1B). Some neuron-related genes, such as *INSM1*,
110 *SEZ6L*, or *SV2B*, were included as their common target genes. On the other hand, we
111 identified 825 SOX2-bound genes (targeted in SBC3) that were specifically occupied in the
112 variant subtype and expressed at higher levels in the variant subtype than in the classical
113 subtypes. Hippo pathway-related genes, such as *YAP1, WWTR1*, *LATS2,* and *REST*, which
114 were not contained in the classical subtypes, were identified in this category (Fig. 1B). To

validate functional differences in SOX2 between the classical and variant subtypes of SCLC, we used the Database for Annotation, Visualization and Integrated Discovery (DAVID) online bioinformatics tool for a GO functional analysis and extracted the top 10 enriched categories in biological processes. Neuron-related categories were more likely to be included in the classical subtype, and cell development- or movement process-related categories in the variant subtype (Fig. 1C). These results suggest that SOX2 regulates distinct transcriptional programs between the classical and variant subtypes of SCLC cell lines.

ASCL1 is one of the driver molecules of SOX2 and recruits SOX2 for distinct transcriptional regulation in classical subtypes of SCLC

To investigate the biological effects of ASCL1 on SOX2 in lung cancer cell lines, we performed *ASCL1* transfection experiments. An A549 cell line that stably expresses ASCL1 was established, as previously reported (Ito *et al.,* 2017; Tenjin *et al.,* 2019). A549 is a representative ADC cell line that does not express ASCL1 or other NE markers. A549 expressed SOX2 more weakly than the SCLC cell lines examined (Fig. 1A). We detected the up-regulated expression of SOX2 following the forced expression of ASCL1 in A549 cells. The expression of INSM1 and WNT11 was also induced (Fig. 2A). Immunohistochemical staining (IHC) revealed that SOX2 was more strongly expressed in xenotransplanted tumor cells

133 with the *ASCL1* transgene than in those from A549 mock cells (Fig. 2B). To show changes in
134 transcriptional regulation driven by SOX2 in an ASCL1-dependent manner, we compared
135 the target genes of SOX2 between *ASCL1*-transfected A549 and A549 mock cells. We
136 combined the results of ChIP- and RNA-seq analyses for these cells and identified 35 genes
137 that had specific SOX2-binding peaks and higher expression levels of mRNAs in
138 *ASCL1*-transfected A549 cells than in mock cells (Fig. 2C). This result suggested that SOX2
139 drives the distinct transcriptional regulation of SCLC. An integrated genome viewer (IGV)
140 snapshot showed SOX2 binding at the overlap region of the transcription start site (TSS) of
141 *INSM1* (Fig. 2D). To confirm that ASCL11 actually affects SOX2 expression in SCLCs, we
142 conducted *ASCL1* knockdown experiments using RNA interference (RNAi) in H69, H889,
143 and SBC1 cell lines as representatives of SCLC cells that simultaneously express ASCL1
144 and SOX2. The knockdown of ASCL1 expression in these cells resulted in significant
145 reductions in SOX2 in 2 out of the 3 cell lines, namely, H889 and SBC1 (Fig.2E).
146 Furthermore, to examine SOX2, ASCL1, and INSM1 expression patterns, we IHC stained
147 30 surgically resected SCLC tissues for these proteins as well as 20 surgically resected ADC
148 and 20 surgically resected SCC tissues for SOX2 and ASCL1. IHC revealed that SCLCs and
149 SCCs expressed SOX2 at slightly higher levels than ADCs: approximately 70.0% in SCLCs,
150 55.0% in SCCs, and 35.0% in ADCs. In SCLC tissues, 60% of cases (18 out of 30 cases) were

151 doubly positive for ASCL1 and SOX2 and were also positive for INSM1. Although
152 SOX2-positive, ASCL1-negative cases were detected (3 out of 30 cases), there were no
153 ASCL1-positive, SOX2-negative cases (0 out of 30 cases). INSM1 was strongly expressed in
154 SCLC (25 out of 30 cases) and all ASCL1-positive cases simultaneously expressed INSM1
155 (18 out of 18 cases) (Fig. 2F, Table 1, and Supplementary Fig. S1). Furthermore, based on
156 the results showing that SOX2, ASCL1, and INSM1 were more likely to be co-expressed in
157 SCLC, we surveyed public datasets of gene expression profiling in human SCLC samples
158 and examined their relationships. The RNA-seq dataset using tumor samples from 79 SCLC
159 patients confirmed the coordinated expression of *ASCL1* and *SOX2* in human SCLC tissue
160 samples (GSE60052: ρ=0.327759, p=0.003168). In the same manner, we confirmed the
161 coordinated expression of *ASCL1* and *INSM1* (GSE60052: ρ=0.357944, p=0.001188).
162 Heatmap data focusing on *SOX2*, *ASCL1*, and *INSM1* was obtained using the dataset
163 reported by Jiang *et al.* (2016) (Fig. 2G). These results support the positive regulation of
164 SOX2 and INSM1 expression by ASCL1.
165
166 **The role of Sox2 in the classical subtype of SCLC cell lines and the *ASCL1*-transfected A549**
167 **cell line**
168 To investigate the biological significance of SOX2 in the classical subtype of SCLC cell

lines and the *ASCL1*-transfected A549 cell line, we conducted *SOX2* knockdown experiments using RNAi on these cells. The knockdown of *SOX2* expression resulted in significant reductions in *ASCL1* (Supplementary Fig. S2) and INSM1 expression (Fig. 3A) in the H69, H889, and SBC1 cell lines. Furthermore, the expression of WNT11 and CDH1 was reduced in the H69, H889, and SBC1 cell lines after the knockdown of SOX2 (Fig. 3A). This result suggests that SOX2 affected EMT in SCLC. The results of the SOX2 knockdown experiment on *ASCL1*-transfected A549 cells were also shown. Not only INSM1 and WNT11, but also NOTCH1, MYC, TCF4, RBL1, and TP53 protein levels decreased after the knockdown of SOX2. The suppression of SOX2 also affected the phosphorylation of histone H3 (p-HH3) protein levels (Fig. 3A). Cell counting assays revealed that the knockdown of *SOX2* suppressed cell growth in the H69, H889, and SBC1 cells lines (Fig. 3B). This result suggests that SOX2 positively affected cell proliferation in the classical subtype of SCLC cells and regulated the expression of key molecules for the SCLC phenotype in the presence of ASCL1.

The role of SOX2 in variant subtypes of SCLC cell lines.

To investigate the role of SOX2 in variant subtypes of SCLC cell lines, we conducted *SOX2* knockdown experiments using RNAi on SBC3 and H69AR cell lines. SBC3 and

187 H69AR are representative variant subtypes of the SCLC cell line that lack the expression of
188 ASCL1 and INSM1. These cells have markedly fewer NE properties than the classical
189 subtype of SCLC cell lines. The results obtained showed that the knockdown of *SOX2* did not
190 significantly reduce tumor cell proliferative capacity in the SBC3 and H69AR cell lines. A
191 quantitative real-time polymerase chain reaction (qRT-PCR) revealed that Hippo-related
192 genes, such as *YAP1* or *TEAD1*, and *VIMENTIN* mRNA expression levels were significantly
193 reduced after the knockdown of *SOX2*. On the other hand, the expression of *ASCL1*, *INSM1*,
194 and *WNT11* was not significantly affected by the knockdown of *SOX2* in these cells (Fig. 4).
195 These results suggest that SOX2 did not always sufficiently affect tumor proliferative
196 capacity in SCLC and, in the variant subtype, it regulated the expression of downstream
197 target genes that were distinct from those of the classical subtype of SCLC. We obtained
198 similar results in the *SOX2* knockout experiments using the CRISPR/Cas9 system on the
199 SBC3 and H69AR cell lines (Supplementary Fig. S3).
200
201 **Ascl1, Sox2, and Insm1 were simultaneously expressed in pulmonary NE tumors in the**
202 **genetically engineered mouse model**
203 The ASCL1 highly-expressing subtype of classical SCLC represents the majority of
204 SCLC based on multiple lines of evidence. ASCL1 is normally present in lung NE cells

during development, and HES1, one of the Notch signaling targets, suppresses the expression of ASCL1 and NE cell differentiation (Borges *et al.,* 1997; Ito *et al.,* 2000). Most of the classical SCLC cell lines and primary tumor samples were shown to strongly express ASCL1 (Rudin *et al.,* 2019). Close signaling contact with the Notch-Hes1 pathway and ASCL1 expression has been proposed to exist in small cell lung carcinogenesis (George *et al.,* 2015). On the other hand, the *Trp53* and *Rb1* double-knockout mouse is fundamentally presented as a gene-engineered SCLC mouse model (Meuwissen *et al.,* 2003). In the present study, we established a *Trp53* -knockout and *Rb1* and *Hes1* double-conditional knockout mouse model, which aimed to add the effects of the inactivation of the Notch-Hes1 pathway to the fundamental SCLC mouse model. The results obtained revealed that multiple SCLC precursor lesions developed in the broncho-bronchiolar epithelium of the mouse and IHC showed that Ascl1, Sox2, and Insm1 were positively expressed in these lesions (Fig. 5). Therefore, the inactivation of Notch signaling induced precursor lesions of the classical subtype of SCLC under *Trp53* - *Rb1* - gene-deficient conditions.

Discussion

SOX2 is an oncogene in human SCLC and its amplification has been detected in some SCLCs. In the present study, we investigated the different functions of SOX2 and whether

223 ASCL1 was present in SCLC cell lines. SOX2 regulated INSM1 or WNT11 with the
224 cooperation of ASCL1 in the classical subtype of SCLC. On the other hand, SOX2 targeted
225 distinct genes, such as the Hippo pathway, in the variant subtype. These results suggest
226 that *SOX2* is not only an oncogene in human SCLC, but may also drive distinct
227 transcriptional regulation in each subtype of SCLC. Therefore, care is needed when
228 considering SOX2 as a potential therapeutic target or biological marker in the diagnosis and
229 treatment of SCLC.

230 We revealed that ASCL1 regulated SOX2 in the classical type of the SCLC cell line.
231 Borromeo et al. (2016) showed that *SOX2* was one of the target genes of ASCL1 in their
232 ChIP-seq of SCLC cell lines, which included H889 SCLC cell lines. Osada *et al.* (2005, 2008)
233 reported roles for ASCL1 in CDH1 expression and NE differentiation. Our results support
234 these findings, and, as a novel insight, ASCL1 and SOX2 cooperatively modulated NE
235 differentiation or EMT in human SCLC. The knockdown of SOX2 expression in the classical
236 subtype of the SCLC cell lines examined resulted in significant reductions in WNT11 and
237 CDH1. In NSCLC, Bartis *et al.* (2013) reported that Wnt11 is a regulator of cadherin
238 expression and related to the function of cellular adhesion. We previously showed that Ascl1
239 induced the EMT-like phenotype in A549 ADC cells (Ito *et al.,* 2017), and demonstrated that
240 WNT11 regulated CDH1 expression in SCLC cell lines (Tenjin *et al.,* 2019). We also

241 confirmed SOX2 binding near the site of the *WNT11* gene in the classical subtype of SCLC
242 cell lines (data not shown). SOX2 may potently modulate NE differentiation and CDH1
243 expression via ASCL1 or WNT11 in SCLC.

244 The results obtained on the knockdown of SOX2 in *ASCL1*-transfected A549 cells are
245 of interest. After the overexpression of ASCL1, SOX2 expression was enhanced and INSM1
246 and WNT11 were simultaneously expressed in this cell. The knockdown of SOX2 in
247 *ASCL1*-transfected cells caused the suppression of INSM1 and WNT11. These results
248 suggest that ASCL1 activates *SOX2* and regulates INSM1 and WNT11 expression together
249 with SOX2. Furthermore, NOTCH1, TCF4, MYC, Trp53, and RBL1 expression decreased
250 after the knockdown of *SOX2* in these cells. Notch signaling is an important cell signaling
251 system, and the interaction between Notch receptors and their ligands induces several genes,
252 such as *HES1*, *CCND1, MYC*, and *AKT* (Rizzo *et al.,* 2008). Intratumoral heterogeneity
253 generated by Notch signaling has been shown to promote SCLC (Lim *et al.,* 2014). The
254 Notch1-Hes1 pathway is a repressor of NE differentiation through the decreased expression
255 of NE-promoting transcription factors, such as ASCL1 and INSM1 (Ito *et al.,* 2000; Ball *et*
256 *al.,* 2004; Hassan *et al.,* 2014; Fujino *et al.,* 2015). Chen *et al.* (2012) reported that silencing
257 of the *SOX2* gene reduced the tumorigenic properties of A549 cells with the attenuated
258 expression of MYC and NOTCH1 in xenografted tumors in the NOD/SCID mouse. The

canonical Wnt pathway induces MYC through TCF4 and other Wnt signal components. In addition, Wnt11 has been reported to activate both canonical and non-canonical Wnt pathways (Stewart *et al.,* 2014; Rapp *et al.,* 2017). Moreover, mouse models carrying conditional alleles for both *Trp53* and *Rb1* developed small cell carcinoma in the lung (Meuwissen *et al.,* 2003). The universal bi-allelic inactivation of *Trp53* and *RB1* was previously reported in human samples (George *et al.,* 2015). Meder *et al.* (2016) showed that NOTCH, ASCL1, Trp53, and RB alterations defined an alternative pathway driving NE and small cell carcinomas. Moreover, the ablation of all three retinoblastoma family members, Rb1, Rbl1, and Rbl2, in the mouse lung resulted in the formation of NE tumors (Lázaro *et al.,* 2017). We demonstrated the induction of precursor SCLC lesions that simultaneously expressed Ascl1, Sox2, and Insm1 in *Trp53 (-/-); CCSPrtTA; tetOCre; Rb1 (fl/fl); Hes1 (fl/fl)* mice. SOX2 has been suggested to play an important role, particularly in an ASCL1-dependent manner, in the SCLC phenotype and tumorigenesis in the interaction with these principle tumor suppressants.

We performed SOX2 knockdown or knockout experiments using RNAi or the CRISPR/Cas9 system in the variant subtype of SCLC, SBC3, and H69AR cells. After the knockdown of *SOX2, YAP1* and *TEAD1* mRNA expression levels decreased in these cells. A previous study reported that YAP1, the main Hippo pathway effector, was frequently lost in

277 high-grade NE lung tumors, and showed reciprocal expression against INSM1 (McColl *et al.,*
278 2017). Among SCLC, the loss of YAP1 correlated with the expression of NE markers, and a
279 survival analysis revealed that YAP1-negative cases were more chemo-sensitive than
280 YAP1-positive cases (Ito *et al.,* 2016). The YAP/TAZ subgroup displayed an adherent cell
281 morphology (Horie *et al.,* 2016) and lower expression levels of ASCL1. *REST* was also
282 included in the genes of SOX2-bound sites in variant subtypes. REST encodes a
283 transcriptional repressor that represses neuronal and NE genes in non-neuronal and
284 non-NE tissues and, thus, serves as a negative regulator of neurogenesis, including SCLC
285 (Gao *et al.,* 2011; Thiel *et al.,* 2015; Lim *et al.,* 2017). We demonstrated that SOX2 modulated
286 the Hippo pathway in the variant subtype of SCLC in the present study. We also showed
287 that *VIMENTIN* mRNA levels decreased after the knockdown of SOX2 in these cells. In the
288 classical subtype of SCLC cell lines, CDH1 expression decreased after the knockdown of
289 SOX2 by RNAi (Fig. 3A). These results suggest that SOX2 potently modulated EMT in lung
290 cancer via the Hippo or Wnt signaling pathway in SCLC.

291 Rudin *et al.* (2012) reported that the knockdown of *SOX2* by doxycycline-inducible
292 shRNA inhibited cell proliferation in SCLC cell lines. In the classical subtype SCLC cell
293 lines, we demonstrated that SOX2-knockdown using RNAi decreased tumor cell
294 proliferative capacity. In contrast, the knockdown of *SOX2* in SBC3 and H69AR cells did not

295 significantly affect their cell proliferative capacity. This functional discrepancy may be
296 attributed to functional differences in Sox2 between the classical and variant subtypes of
297 SCLC. Furthermore, Rudin *et al.* (2019) recently proposed a nomenclature to describe SCLC
298 subtypes according to the dominant expression of transcription factors. They divided SCLC
299 into 4 subtypes, which considered the master regulators of SCLC; ASCL1, NEUROD1,
300 POU2F3, or YAP1. In the present study, we revealed that SOX2 cooperated with the key
301 regulatory molecules, such as ASCL1 and YAP1, in SCLC, and showed that SCLC may be
302 divided into 3 groups based on the expression of ASCL1 and SOX2; ASCL1-SOX2 doubly
303 high, ASCL1 low and SOX2 high, and ASCL1-SOX2 doubly low (Fig. 6). In addition to
304 genomic profiling, which has been adopted in clinical practice, several research initiatives to
305 catalog DNA, RNA, and protein profiles among lung SCC and ADC have accelerated the
306 pace of discovery, such as The Cancer Genome Atlas (TCGA). However, similar efforts have
307 not yet been achieved for SCLC due to the lack of adequate tumor tissue (Byers *et al.,* 2015).
308 This needs to be investigated in a large prospective or cohort study in the future.

309 In summary, the classical subtype of SCLC frequently and strongly expresses both
310 SOX2 and ASCL1. ASCL1-recruited SOX2 plays an important role in driving distinct
311 transcriptional regulation. We demonstrated that SOX2 regulates lineage-specific genes,
312 such as *INSM1*, in the classical subtype of SCLC. While we revealed the significance of

SOX2 for cell growth and the modulation of EMT, we detected a functional discrepancy in SOX2 between the classical and variant subtypes of SCLC. The present results suggest that the ASCL1-SOX2 axis is extremely important as a potential therapeutic target or biological marker in the classical subtype of SCLC. On the other hand, the fundamental role of SOX2 in the variant subtype, in which ASCL1 is negative, was shown in the activation of the Hippo signaling pathway. Further studies on SOX2 that focus on highly specific molecules, for example, those that are involved in the recruitment of SOX2 in the variant subtype of SCLC, are needed. The present study promotes our understanding of the significance of SOX2 in SCLC, which will hopefully lead to the development of novel targeted therapies and better prognoses for patients with SCLC.

Materials and Methods

Cell Lines

Seven SCLC cell lines (H69, H889, SBC1, H69AR, H1688, SBC3, and SBC5), 3 ADC cell lines (A549, H358, and H1975), and 2 SCC cell lines (H2170 and H226) were used in the present study. H69, H889, H69AR, H1688, A549, H358, H1975, H2170, and H226 were purchased from ATCC (Manassas, VA), and SBC1, SBC3, and SBC5 from the Japan Collection of Research Bioresources Cell Bank (Osaka, Japan). All growth media were

purchased from Wako Pure Chemical Industries Ltd. (Osaka, Japan) and supplied with 1% penicillin/streptomycin (Sigma–Aldrich, Ontario, Canada). A549 cells were grown in DMEM supplemented with 10% FBS (Hyclone, Logan, UT). SBC-3 cells were grown in EMEM with 10% FBS. H69, H1688, and H2170 cells were grown in RPMI 1640 medium supplemented with 2 mM L-glutamine, 10 nM HEPES, 1 mM sodium pyruvate, 4.5 g/L glucose, 1.5 g/L sodium bicarbonate, and 10% FBS. H69AR cells were grown in similar RPMI 1640 medium, but supplemented with 20% FBS. All cells were incubated at 37 °C in 5% CO_2 and saturated humidity. Cells were maintained as subconfluent cultures before use and harvested with trypsin-EDTA (Invitrogen, Carlsbad, CA).

Tissue Samples

We obtained tissue samples of SCLCs (n=30), ADCs (n=20), and SCCs (n=20) from the lung cancer files of the Department of Pathology and Experimental Medicine of Kumamoto University and resected at the Department of Thoracic Surgery of Kumamoto University from 70 patients for this study. A histological diagnosis of the samples was made according to the criteria of the WHO (Travis *et al.,* 2015). These sections were used for IHC staining. The present study followed the guidelines of the Ethics Committee of Kumamoto University.

349 **WB Analysis**

350 Cells were prepared for a WB analysis as previously described (Yoshida *et al.,* 2013). A
351 list of the primary antibodies used is shown in Table 2. Membranes were washed and
352 incubated with the respective secondary antibodies conjugated with peroxidase (Amersham
353 Pharmacia Biotech, Buckinghamshire, UK) for 1 hour, and the immune complex was
354 visualized with the chemiluminescence substrate (Amersham Pharmacia Biotech, UK).

355

356 **ChIP**

357 Three SCLC cell lines (H69, H889, and SBC3), A549 ADC cell lines, and an A549 cell
358 line with the stable expression of ASCL1 were used in the present study. Cells were fixed in
359 1% formaldehyde (Thermo-Fisher) in PBS at room temperature for 10 minutes. Crosslinked
360 cells were lysed with LB1 (50 mM HEPES-KOH (pH7.5), 140 mM NaCl, 1 mM EDTA, 10%
361 (w/v) glycerol, 0.5% (w/v) NP-40, 0.25% (w/v) TritonX-100, proteinase inhibitor cocktail
362 (Sigma)) and washed with LB2 (10 mM Tris-HCl (pH 8.0), 200 mM NaCl, 1 mM EDTA, 0.5
363 mM EGTA, proteinase inhibitor cocktail). Chromatin lysates were prepared in RIPA buffer
364 (Thermo 89900; 25 mM Tris-HCl pH7.6, 150 mM NaCl, 0.1% SDS, 1% NP-40, 1% sodium
365 deoxycolate, proteinase inhibitor cocktail), sonication with Covaris S220 (Peak Incident
366 Power, 175：Acoustic Dutu Factor, 10%：Cycle Per Burst, 200：Treatment time, 600sec：

Cycle, 6). ChIP was performed using chromatin lysates equivalent to 1.0 × 10 7 cells, and protein A Dyna-beads (Thermo-Fisher) coupled with the antibody against Sox2 (raised by us). After 4 hours of incubation at 4 °C, beads were washed 4 times in a low salt buffer (20 mM Tris-HCl (pH 8.0), 0.1% SDS, 1% (w/v) TritonX-100, 2 mM EDTA, 150 mM NaCl), and two times with a high salt buffer (20 mM Tris-HCl (pH 8.0), 0.1% SDS, 1% (w/v) TritonX-100, 2 mM EDTA, 500 mM NaCl). Chromatin complexes were eluted from the beads by agitation in elution buffer (10 mM Tris-HCl (pH 8.0), 300 mM NaCl, 5 mM EDTA, 1% SDS) and incubated overnight at 65 °C for reverse-crosslinking. Eluates were treated with RNase A and Proteinase K, and DNA was ethanol precipitated.

ChIP -seq data analysis

ChIP-seq libraries were prepared using 20 ng of input DNA, and 1-3 ng of ChIP DNA with KAPA Library Preparation Kit (KAPA Biosystems) and NimbleGen SeqCap Adaptor Kit A or B (Roche) and sequenced by Illumina NextSeq 500 (Illumina) using Nextseq 500/550 High Output v2 Kit (Illumina) to obtain single end 75-nt reads. The resulting reads were trimmed to remove the adapter sequence and low-quality ends using Trim Galore! v0.4.3 (cutadapt v.1.15). The trimmed ChIP-seq reads were mapped to the UCSC hg38 genome assemblies using Bowtie2 v2.3.3 with default parameters. The resulting SAM files

were converted to the BAM format using SAMtools v1.5. Peak calling was performed using MACS2 v2.1.1. with input DNA as a control including a q-value cut-off of 0.01 for SOX2 ChIP-seq. The distance to the nearest TSS and gene feature of the peaks were obtained from Ensembl human annotation data (GRCh38) using the annotatePeakInBatch of ChIPpeakAnno and biomaRt R packages. Peaks in the gene body were first annotated with the option 'output="overlapping", and the remained peaks were then annotated to the nearest TSSs regardless of the distance between them. Protein binding sites were shown along with genomic loci from RefSeq genes on the genome browser IGV.

RNA sequence (RNA-seq)

RNA-seq was performed by the Liaison Laboratory Research Promotion Center (LILA) (Kumamoto University) as follows. Total RNA was isolated using the RNeasy Mini Kit (Qiagen, Germany). 2100 Bioanalyzer was used to detect the concentration and purity of total RNA. All samples with an RNA integrity number (RIN) >7.5 were used for sequencing. Library DNA prepared according the Illumina Truseq protocol using Truseq Standard mRNA LT Sample Prep Kits and sequenced by Nextseq 500 (Illumina) was used for analysis, and the data were converted to Fastq files. Quality control of the data was performed by FastQC. The reads were then trimmed to remove the adapter sequence using Trim Galore!

v0.5.0 (Cutadapt v 1.16), and low-quality reads were filtered out using FASTX-toolkit v0.0.14. The remaining reads were aligned to the Ensembl GRCh38.93 reference genome using STAR ver.2.6.0a. FPKM (fragments per kilobase of exon per million reads mapped) values were calculated using Cuffdiff. Significant genes were extracted by cuffdiff ($p<0.05$). A differential expression analysis was performed using the ExAtlas website (https://lgsun.irp.nia.nih.gov/exatlas/).

Gene ontology (GO) analysis

GO annotation and classification were based on three categories, including biological process, molecular function, and cellular component. The Database for Annotation, Visualization, and Integrated Discovery Bioinformatics Resources 6.7 (DAVID 6.7, http://www.david.niaid.nih.gov) was used for the GO analysis (Huang *et al.,* 2009). The gene lists contained significant genes in the RNA-seq analysis and were also targeted by Sox2 in our ChIP-seq analysis. To visualize key biological processes, the DAVID online database was used. The top 10 categories in each classical and variant subgroup of SCLC were taken as excerpts for Fig. 1C.

Transfection with siRNA

421 We purchased Sox2 siRNA (sc-41120) and Ascl1 siRNA (sc-37692) from Santa Cruz
422 Biotechnology (Santa Cruz, USA) and transfected them into cells using an electroporator
423 (NEPA21 pulse generator; Nepa Gene, Chiba, Japan) as described in the manufacturer's
424 instructions. These were a pool of 3 different siRNA duplexes and sequences for Sox2 were
425 as follows. sense; 5'-GAAUGGACCUUGUAUAGAUTT -3', antisense;
426 5'-AUCUAUACAAGGUCCAUUCTT -3' (sc-38408A), sense; 5' –
427 GGACAGUUGCAAACGUGAATT -3', antisense; 5'-UUCACGUUUGCAACUGUCCTT -3'
428 (sc-38408B), and sense; 5'-GAAUCAGUCUGCCGAGAAUTT -3', antisense; 5'-
429 AUUCUCGGCAGACUGAUUCTT -3' (sc-41120C). The sequences for Ascl1 were as follows.
430 sense; 5'-CCAACAAGAAGAUGAGUAATT-3', antisense;
431 5'-UUACUCAUCUUCUUGUUGGTT-3' (sc-37692A), sense; 5'-
432 GAAGCGCUCAGAACAGUAUTT-3', antisense; 5'- AUACUGUUCUGAGCGCUUCTT-3'
433 (sc-37692B), sense; 5'- GUUCGGGGAUAUAUUAAGATT-3', antisense; 5'-
434 UCUUAAUAUAUCCCCGAACTT-3' (sc-37692B). Control siRNA (Cat# sc-36869) was used
435 as a control. Cells were harvested 48-72 h post-transfection.
436
437 **Plasmid construction and transfection**
438 To construct pCAG-IRES-puro-FlagHA, we replicated the *ASCL1* gene of a human

ASCL1 cDNA ORF clone and replaced it with *ASCL1*. We generated pCAG-IRES-puro-FlagHA -mock from a human *ASCL1* cDNA ORF clone by cleaving out *ASCL1*. Two plasmids were transfected into A549 cells with Lipofectamine 3000 (Invitrogen) as described in the manufacturer's instructions. After 48 h, 1 μg/mL of puromycin (Clontech) was added to cells for 2 weeks, with a medium change every 3 days. Stably transfected resistant cell lines were cloned from each transfectant.

Cell counting assay

A cell counting method was used to evaluate the role of Sox2 in cell proliferation. After 48 h of siRNA and control transfection, cells were stained with trypan blue and counted. H69, H889, and SBC1 cells were used and seeded at 2×10^5 cells on 6-well plates. Every 2 days, cells were collected and counted, after which they were seeded into new fresh medium and left at 37 °C in 5% CO_2. The counting method was continued until day 6. The criteria for cellular integrity included trypan blue exclusion, an intact nucleus, and intact cell membrane. Experiments were repeated three times separately to confirm reproducibility.

IHC and evaluation

456 Formalin-fixed, paraffin-embedded specimens were cut into 4-µm-thick sections and
457 mounted onto MAS-GP–coated slides (Matsunami Glass Ind., Osaka, Japan). After being
458 deparaffinized and rehydrated, sections were heated using an autoclave in 0.01 mol/L
459 citrate buffer (pH 7.0) for antigen retrieval. Sections were incubated with 0.3% H_2O_2 in
460 absolute methanol for 30 minutes to block endogenous peroxidase activity. Sections were
461 then incubated with skimmed milk for 30 minutes to block non-specific staining. After this
462 blocking step, sections were incubated with the primary antibodies shown in Table 2 at 4°C
463 overnight. This was followed by sequential 1-hour incubations with the secondary antibodies
464 (En Vision+ System-HRP-Labeled Polymer; Dako) and visualization with the Liquid DAB+
465 Substrate Chromogen System (Dako). All slides were counterstained with hematoxylin for
466 30 seconds before being dehydrated and mounted. We evaluated IHC results based on
467 staining intensity and the percentage of positively stained tumor cells. The percentage of
468 positively stained tumor cells was divided into five groups: no staining, <5% tumor cells
469 reactive, 5–25% reactive, 25-50% reactive, and >50% reactive. The staining intensity level
470 was divided into three groups: negative, weak, and strong. We designed a table to allocate
471 IHC scores to each specimen. IHC scores were classified into three groups: negative (0),
472 weak positive (1+), and positive (2+). We defined a 2+ IHC score as significantly positive.

Scoring was simultaneously performed by two independent observers who were blinded to patient details.

qRT-PCR

Total RNA was isolated using an RNeasy Mini Kit (Qiagen, Germany) in accordance with the manufacturer's instructions. cDNA was produced using a ReverTra Ace qPCR RT-kit (Toyobo, Osaka, Japan), according to the manufacturer's instructions. A list of the primers used is shown in Table 3. cDNA was subjected to quantitative SYBR Green real-time PCR by using SYBR Premix Ex Taq II (Takara Bio). A list of the specific primers used is shown in Table 3. qRT-PCR was performed with a LightCycler® Nano (Roche Diagnostic K.K.) using 40 cycles of a three-stage program with the following conditions: 20 seconds at 94°C, 40 seconds at 60°C, and 15 seconds at 72°C, as recommended by the manufacturer. The products were quantified during the initial exponential phase of amplification above the baseline. Data were obtained from triplicate reactions. The means and SDs of the copy numbers were normalized to the value for *glyceraldehyde-3-phosphate dehydrogenase* (*GAPDH*) mRNA.

***SOX2*-knockout experiment using SBC3 and H69AR cell lines**

Genome editing using CRISPR/Cas9 was used for the knockout of the *SOX2* gene in the SBC3 and H69AR cell lines. We purchased a *SOX2*-knockout vector from GeneCopoeia™ (Rockville, USA). These were 3 different human SOX2 sgRNA/Cas9 all-in-one expression clones (NM_003106.2). The sgRNA target sequences of *SOX2* were as follows: ATGGGCCGCTTGACGCGGTC (HCP217628-CG10-3-10-a), CGCCCGCATGTACAACATGA (HCP217628-CG10-3-10-b), and ATTATAAATACCGGCCCCGG (HCP217628-CG10-3-10-c). CCPCTR01-CG10 (GeneCopoeia™) was used as a control. The sgRNA target sequence was as follows: GGCTTCGCGCCGTAGTCTTA. Regarding the establishment of *SOX2*-knockout H69AR cells, we obtained pSpCas9(BB)-2A-Puro(px459) from Addgene (Cambridge, MA) (Ran *et al.,* 2013). The sgRNA target sequences of *SOX2* were as follows: ATAATAACAATCATCGGCGG, GACCGCGTCAAGCGGCCCAT and ACAGCCCGGACCGCGTCAAG. Cells were harvested 48-72 hr post-transfection. These plasmids were co-transfected with Lipofectamine 3000 (Thermo Fisher Scientific) into cells at subconfluency. After 48 hr, transfected cells were treated with 200 μg/mL hygromycin B (Nacalai Tesque, Kyoto, Japan) or 1 μg/mL puromycin (Clontech) for the selection of stably transfected cells.

Tumor xenotransplantation experiment

509 Eight-week-old male Rag2(−/−);Jak3(−/−) mice (a generous gift from Prof. S. Okada;
510 Kumamoto University) were used. Two groups of mice were subcutaneously injected; one
511 group was injected with 2×10^6 stably transfected cells with *ASCL1*, and the other group
512 was injected with an equal number of the control cell population. After 4 weeks,
513 subcutaneous tumors were removed and fixed. The samples were fixed with 10% formalin
514 and embedded in paraffin. Tissue sets were stained with hematoxylin and eosin and
515 additional sections were used for IHC staining. Regarding tumor xenograft growth, a total of
516 1.0×10^6 cells each of the mock-transfected and *SOX2* knockout SBC3 cell lines and mock
517 cells were subcutaneously injected into the backs of mice. Twenty days after the first
518 injection, tumors were removed and measured. All animal experiments were performed in
519 accordance with the Institutional Animal Care and Use Committee guidelines.
520
521 **_In situ_ precursor SCLC model mouse**
522 We established a genetically engineered mouse model for *in situ* SCLC precursor
523 lesions. These mice are *Trp53* gene-deficient, have Clara cell secretory protein promoter
524 (CCSP) rt TA, tetO Cre-recombinase, floxed *Rb1*, and floxed *Hes1* genes, and were kept
525 under the hypothesis that tumorigenesis of SCLC may occur with the double knockout of the
526 suppressor oncogenes, *p53* and *Rb1*, and inactivation of the Notch signal pathway (Meder *et*

527 *al.,* 2016). *P53* KO mice (ICR.Cg.-*Trp53*<tm1Sia>/Rbrc) (Tsukuda T *et al.,* 1993) were
528 obtained from the Riken BioResource Center (Tsukuba, Japan), CCSPrtTA; tetOCre mice
529 (Tichelarr *et al.,* 2002) were a generous gift from Dr. J. Whitsett. Floxed *Rb1* mice
530 (FVB;129-Rb1^{tm2Brn}/Nci; Vooijs *et al.,* 1999) were obtained from the NCI Mouse Repository
531 (Frederick, MD), and floxed *Hes1* mice (Imayoshi *et al.,* 2008) from Dr. R. Kageyama of
532 Kyoto University. Animals were kept under standard laboratory conditions with free access
533 to water and food, and were maintained on a 12-h light/dark cycle under pathogen-free
534 conditions. Doxycycline (Sigma-Aldrich) was dissolved in drinking water at a concentration
535 of 1 g/L, and given to 4-week-old male animals for 6 weeks. After the treatment with
536 doxycycline, animals were sacrificed with an intraperitoneal injection of an overdose of
537 pentobarbital, and lung tissues were fixed in phosphate-buffered fixed 4%
538 paraformaldehyde for 1 week. Fixed lung tissues were embedded in paraffin, and paraffin
539 sections were used for hematoxylin eosin staining and immunostaining for Ascl1, Sox2, and
540 Insm1. The present study was approved by the Animal Care Committee of Kumamoto
541 University (#A2019-038).
542
543 **Statistical analysis**
544 Spearman's correlation coefficient (ρ) was calculated for the correlation analysis. Cell

545 counting data were expressed as the means ± standard deviation of triplicate measurements.
546 Differences in mean values between the groups were analyzed by a two-tailed statistical
547 analysis using the Student's *t*-test. GraphPad Prism version 7.04 (San Diego, CA) was used
548 for the statistical analysis. *p* values less than 0.05 were considered to be significant.

549 **Dataset availability**

550 The dataset produced in this study is available in the following database:

551 ・RNA-seq data: Gene Expression Omnibus GSE60052
552 (https://www.ncbi.nlm.nih.gov/geo/query/acc.cgi?acc=GSE60052)

553

554 **References**

555 Ball DW, Azzoli CG, Baylin SB, Chi D, Dou S, Donis-Keller H, Cumaraswamy A, Borges M,
556 Nelkin BD (1993) Identification of a human achaete-scute homolog highly expressed
557 in neuroendocrine tumors. Proc Natl Acad Sci U S A 90: 5648-52
558 Ball DW (2004) Achaete-scute homolog-1 and Notch in lung neuroendocrine development
559 and cancer. Cancer Lett 204: 159-69
560 Bartis D, Csongei V, Weich A, Kiss E, Barko S, Kovacs T, Avdicevic M, D'Souza VK, Rapp J,
561 Kvell K, Jakab L, Nyitrai M, Molnar TF, Thickett DR, Laszlo T, Pongracz JE (2013)

562 Down-Regulation of Canonical and Up-Regulation of Non-Canonical Wnt Signalling
563 in the Carcinogenic Process of Squamous Cell Lung Carcinoma. PLos One 8: e57393.7
564 Borges M, Linnoila RI, van de Velde HJ, Chen H, Nelkin BD, Mabry M, Baylin SB, Ball DW
565 (1997) An achaete-scute homologue essential for neuroendocrine differentiation in the
566 lung. Nature 386: 852-6
567 Borromeo MD, Savage TK, Kollipara RK, He M, Augustyn A, Osborne JK,Girard L, Minna
568 JD[6], Gazdar AF[7], Cobb MH[8], Johnson JE (2016) ASCL1 and NEUROD1 Reveal
569 Heterogeneity in Pulmonary Neuroendocrine Tumors and Regulate Distinct Genetic
570 Programs. Cell Rep 16: 1259-72
571 Byers LA, Rudin CM. Small cell lung cancer: where do we go from here? (2015) Cancer 121:
572 664-72
573 Carney DN, Gazdar AF, Bepler G, Guccion JG, Marangos PJ, Moody TW, Zweig MH, Minna
574 JD (1985) Establishment and identification of small cell lung cancer cell lines having
575 classic and variant features. Cancer Res 45: 2913-23
576 Chen S, Xu Y, Chen Y, Li X, Mou W, Wang L, Liu Y, Reisfeld RA, Xiang R, Lv D, Li N (2012)
577 SOX2 gene regulates the transcriptional network of oncogenes and affects
578 tumorigenesis of human lung cancer cells. PLos ONE 7: e36326

579 Fujino K, Motooka Y, Hassan WA, Ali Abdalla MO, Sato Y, Kudoh S, Hasegawa K,
580 Niimori-Kita K, Kobayashi H, Kubota I, Wakimoto J, Suzuki M, Ito T (2015) INSM1 is
581 a crucial regulator of neuroendocrine differentiation in lung cancer. Am J Pathol 185:
582 3164–77

583 Gao Z, Ure K, Ding P, Nashaat M, Yuan L, Ma J, Hammer RE, Hsieh J (2011) The master
584 negative regulator REST/NRSF controls adult neurogenesis by restraining the
585 neurogenic program in quiescent stem cell. J Neurosci 31: 9772-86

586 Gazdar AF, Bunn PA, Minna JD (2017) Small-cell lung cancer: what we know, what we
587 need to know and the path forward. Nat Rev Cancer 17: 765

588 Gazdar AF, Carney DN, Nau MM, Minna JD (1985) Characterization of variant subclasses
589 of cell lines derived from small cell lung cancer having distinctive biochemical,
590 morphological, and growth properties. Cancer Res 45: 2924-30

591 George J, Lim JS, Jang SJ, Cun Y, Ozretić L, Kong G, Leenders F, Lu X, Fernández-Cuesta
592 L, Bosco G, Müller C, Dahmen I, Jahchan NS, Park KS, Yang D, Karnezis AN, Vaka D,
593 Torres A, Wang MS, Korbel JO et al (2015) Comprehensive genomic profiles of small
594 cell lung cancer. Nature 524: 47-53.

595 Hassan WA, Yoshida R, Kudoh S, Hasegawa K, Niimori-Kita K, Ito T (2014) Notch1 controls
596 cell invasion and metastasis in small cell lung carcinoma cell lines. Lung Cancer 86:
597 304-10
598 Horie M, Saito A, Ohshima M, Suzuki HI, Nagase T (2016) YAP and TAZ modulate cell
599 phenotype in a subset of small cell lung cancer. Cancer Sci 107: 1755-1766
600 Huang DW, Sherman BT, Lempicki RA (2009) Systematic and integrative analysis of large
601 gene lists using DAVID bioinformatics resources. Nature Protoc 4: 44-57
602 Imayoshi I, Shimogori T, Ohtsuka T, Kageyama R (2008) Hes genes and neurogenin regulate
603 non-neural versus neural fate specification in the dorsal telencephalic midline.
604 Development 135:2531-2541
605 Ito T, Kudoh S, Ichimura T, Fujino K, Hassan WA, Udaka N (2017) Small cell lung cancer, an
606 epithelial to mesenchymal transition (EMT)-like cancer: significance of inactive Notch
607 signaling and expression of achaete-scute complex homologue 1. Hum Cell 30: 1-10
608 Ito T, Matsubara D, Tanaka I, Makiya K, Tanei ZI, Kumagai Y, Shiu SJ, Nakaoka HJ,
609 Ishikawa S, Isagawa T, Morikawa T, Shinozaki-Ushiku A, Goto Y, Nakano T, Tsuchiya
610 T, Tsubochi H, Komura D, Aburatani H, Dobashi Y, Nakajima J (2016) Loss of YAP1
611 defines neuroendocrine differentiation of lung tumors. Cancer Sci 107: 1527-38

612 Ito T, Udaka N, Yazawa T, Okudela K, Hayashi H, Sudo T, Guillemot F, Kageyama R,
613 Kitamura H (2000) Basic helix-loop-helix factors regulate the neuroendocrine
614 differentiation of fetal mouse pulmonary epithelium. Development 127: 3913–21
615 Jiang L, Huang J, Higgs BW, Hu Z, Xiao Z, Yao X, Conley S, Zhong H, Liu Z, Brohawn P,
616 Shen D, Wu S, Ge X, Jiang Y, Zhao Y, Lou Y, Morehouse C, Zhu W, Sebastian Y,
617 Czapiga M (2016) Genomic landscape survey identifies SRSF1 as a key oncodriver in
618 small cell lung cancer. PLoS Genet 12: e1005895
619 Lim JS, Ibaseta A, Fischer MM, Cancilla B, O'Young G, Cristea S, Luca VC, Yang D,
620 Jahchan NS, Hamard C, Antoine M, Wislez M, Kong C, Cain J, Liu YW, Kapoun AM,
621 Garcia KC, Hoey T, Murriel CL, Sage J (2017) Intratumoural heterogeneity generated
622 by Notch signaling promotes small-cell lung cancer. Nature 545: 360-364
623 Lázaro S, Pérez-Crespo M, Enguita AB, Hernández P, Martínez-Palacio J, Oteo M, Sage J,
624 Paramio JM, Santos M (2017) Ablating all three retinoblastoma family members in
625 mouse lung leads to neuroendocrine tumor formation. Oncotarget 8: 4373-4386
626 McColl K, Wildey G, Sakre N, Lipka MB, Behtaj M, Kresak A, Chen Y, Yang M, Velcheti V,
627 Fu P, Dowlati A (2017) Reciprocal expression of INSM1 and YAP1 defines subgroups
628 in small cell lung cancer. Oncotarget 8: 73745-73756.
629 Meder L, König K, Ozretić L, Schultheis AM, Ueckeroth F, Ade CP, Albus K, Boehm D,

630 Rommerscheidt-Fuss U, Florin A, Buhl T, Hartmann W, Wolf J, Merkelbach-Bruse S,
631 Eilers M, Perner S, Heukamp LC, Buettner R (2016) NOTCH, ASCL1, p53, and RB
632 alterations define an alternative pathway driving neuroendocrine and small cell
633 carcinomas. Int J Cancer 138: 927-38
634 Meuwissen R, Linn SC, Linnoila RI, Zevenhoven J, Mooi WJ, Berns A (2003) Introduction of
635 small cell lung cancer by somatic inactivation of both Trp53 and Rb1 in a conditional
636 mouse model. Cancer Cell 4:181-9
637 Osada H, Tatematsu Y, Yatabe Y, Horio Y, Takahashi T (2005) ASH1 gene is a specific
638 therapeutic target for lung cancers with neuroendocrine features. Cancer Res 65:
639 10680-5
640 Osada H, Tomida S, Yatabe Y, Tatematsu Y, Takeuchi T, Murakami H, Kondo Y, Sekido Y,
641 Takahashi T (2008) Roles of achaete-scute homologue 1 in DKK1 and E-cadherin
642 repression and neuroendocrine differentiation in lung cancer. Cancer Res 68: 1647-55
643 Ran F, Hsu PD, Wright J, Agarwala V, Scott DA, and Zhang F (2013) Genome engineering
644 using the CRSPR-Cas9 system. Nat Protoc 8: 2281-2308
645 Rapp J, Jaromi L, Kvell K, Miskei G, Pongracz JE (2017) WNT signaling - lung cancer is no
646 exception. Respir Res 18:167

647 Rizzo P, Osipo C, Foreman K, Golde T, Osborne B, Miele L (2008) Rational targeting of Notch
648 signaling in cancer. Oncogene 27: 5124-31
649 Rudin CM, Durinck S, Atawiski F, Poirier JT, Modrusan Z, Shames DS, Bergbower EA,
650 Guan Y, Shin J, Guillory J, Rivers CS, Foo CK, Bhatt D, Stinson J, Gnad F, Haverty
651 PM, Gentleman R, Chaudhuri S, Janakiraman V, Jaiswal BS et al (2012)
652 Comprehensive genomic analysis identifies SOX2 as a frequently amplified gene in
653 small-cell lung cancer. Nat Genet 44: 1111-6
654 Rudin CM, Poirier JT, Byers LA, Dive C, Dowlati A, George J, Heymach JV, Johnson JE,
655 Lehman JM, MacPherson D, Massion PP, Minna JD, Oliver TG, Quaranta V, Sage J,
656 Thomas RK, Vakoc CR, Gazdar AF (2019) Molecular subtypes of small cell lung
657 cancer: a synthesis of human and mouse model data. Nat Rev Cancer 19: 289-297
658 Stewart DJ (2014) Wnt signaling pathway in non-small cell lung cancer. J Natl Cancer Inst
659 106:djt356
660 Tenjin Y, Kudo S, Kubota S, Yamada T, Matsuo A, Sato Y, Ichimura T, Kohrogi H, Sashida G,
661 Sakagami T, Ito T (2019) Ascl1-induced Wnt11 regulates neuroendocrine
662 differentiation, proliferation and E-cadherin expression in small-cell lung cancer and
663 Wnt11 regulates small-cell lung cancer biology. Lab Invest doi:
664 10.1038/s41374-019-0277-y.

665 Thiel G, Ekici M, Rossler OG (2015) RE-1 silencing transcription factor (REST): a regulator
666 of neuronal development and neuronal/endocrine function. Cell Tissue Res 359:
667 99-109

668 Tichelarr J, Lu W, Whitsett J (2002), Conditional expression of fibroblast growth factor-7 in
669 the developing and mature lung. J Biol Chem 275:11858-11864

670 Travis WD, Brambilla E, Burke AP, Marx, A., Nicholson, A. G (2015) WHO classification of
671 tumours of the lung, pleura, thymus and heart, 4th ed. Lyon, France, IARC, 63-68

672 Tsukuda T, Tomooka Y, Takai S, Ueda Y, Nishikawa S, Yagi T, Tikunnaga T, Takeda N, Suda
673 Y, Abe S (1993) Enhanced proliferative potential in culture of cells from p53-deficient
674 mice. Oncogene 8:3313-3322

675 Vooijs M, Berns A (1999) Developmental defects and tumor predisposition in Rb mutant
676 mice. Oncogene 18: 5293-303.

677 Wael H, Yoshida R, Kudoh S, Hasegawa K, Niimori-Kita K, Ito T (2014) Notch1 signaling
678 controls cell proliferation, apoptosis and differentiation in lung carcinoma. Lung
679 Cancer 85: 131–40

680 Wang S, Tang J, Sun T, Zheng X, Li J, Sun H, Zhou X, Zhou C, Zhang H, Cheng Z, Ma H,
681 Sun H (2017) Survival changes in patients with small cell lung cancer and disparities
682 between different sexes, socioeconomics statues and ages. Sci Rep 7: 1339

683 Yoshida R, Nagata M, Nakayama H, Niimori-Kita K, Hassan W, Tanaka T, Shinohara M, Ito
684 T (2013) The pathological significance of Notch1 in oral squamous cell carcinoma. Lab
685 Invest 93: 1068-81
686 Zhang W, Girard L, Zhang YA, Haruki T, Papari-Zareei M, Stastny V, Ghayee HK, Pacak K,
687 Oliver TG, Minna JD, Gazdar AF (2018) Small cell lung cancer tumors and preclinical
688 models display heterogeneity of neuroendocrine phenotypes. Transl Lung Cancer Res
689 7: 32-49

690

691 **Acknowledgments**

692 We thank Ms. Yuko Fukuchi and Ms. Takako Maeda for their technical assistance; the
693 staff of LILA for their technical support; the Institute of Molecular Embryology and Genetics,
694 Kumamoto University for its help with the RNA-seq analysis. This study was partially
695 supported by a Grant-in-Aid for Scientific Research from the Ministry of Education, Culture,
696 Sports, Science and Technology of Japan 18K19480 and by Aihara Pediatric and Allergy
697 Clinic, Yokohama, Japan. This study was also supported in part by the program of the Joint
698 Usage/Research Center for Developmental Medicine, Institute of Molecular Embryology and
699 Genetics, Kumamoto University.

700

Conflicts of interest

We have no conflicts of interest to disclose.

Figure legends

Fig. 1: (A) WB analysis of SOX2, ASCL1, and INSM1 in lung cancer cell lines, including small cell lung carcinoma (SCLC), adenocarcinoma (ADC), and squamous cell carcinoma (SCC). SOX2 was more strongly expressed in all SCLC cell lines than in the NSCLCs examined. Four out of the 7 SCLC cell lines simultaneously expressed ASCL1 and INSM1. ß-ACTIN served as an internal control. (B) ChIP-seq and RNA-seq were conducted to analyze putative SOX2 target genes and mRNA expression in the H69, H889, and SBC3 cell lines. As shown in a Venn plot, 346 specific SOX2-bound genes, which also significantly expressed mRNAs in the classical subtype, were identified (shared in NCI-H69 and NCI-H889). *INSM1* was included as a common gene. In a similar manner, 825 specific SOX2-bound genes that also significantly expressed mRNAs were identified in the variant subtype of the SBC3 cell line. Hippo pathway-related genes and *REST* were included as common genes. (C) Results of the GO functional analysis. The top 10 enriched categories in biological processes in each of the classical and variant subgroups were shown. The distinct functions of SOX2 in each subgroup were suggested.

719

720 Fig. 2: (A) A WB analysis showed that the transfection of *ASCL1* in A549 ADC cells
721 increased SOX2, INSM1 and WNT11 expression. ß-ACTIN served as an internal control. (B)
722 Tumor tissues by the xenotransplantation of mock A549 cells and *ASCL1*-transfected A549
723 cells in immunodeficient mice. Using IHC, *ASCL1* transfection induced SOX2 protein
724 expression in tumor cell nuclei. Representative images are shown. Scale bar = 200 µm. (C)
725 Changes in transcriptional regulation driven by SOX2 between *ASCL1*-transfected A549
726 and A549 mock cells. ChIP- and RNA-seq combined data showed 35 specific SOX2-bound
727 genes in *ASCL1*-transfected A549. *INSM1* was newly detected after the transfection of
728 *ASCL1.* (D) An integrated genome viewer (IGV) snapshot showed SOX2 binding at the
729 overlap region of the transcription starting site and ASCL1 binding near the site of the
730 *INSM1* gene in SCLC cell lines. (E) The suppression of SOX2 by RNAi for ASCL1 was
731 confirmed in H889 and SBC1 cells by a WB analysis (F) IHC images of surgically resected
732 SCLC tissues for SOX2, ASCL1, and INSM1. These proteins were strongly expressed in
733 tumor cell nuclei. Representative images are shown. Scale bar = 200 µm. (G) Expression
734 levels of *ASCL1*, *INSM1*, and *SOX2* in the RNA-seq dataset of SCLC tissues. The GSE60052
735 (n=79) dataset (Jiang *et al.,* 2016) was analyzed. NT, non-treated; si, small interfering.

736

737 Fig. 3: (A) SOX2 affects INSM1, WNT11, and CDH1 expression in SCLC cell lines. The
738 suppression of INSM1, WNT11, and CDH1 was observed in the classical subtype of the
739 SCLC cell lines, H69, H889, and SBC1s with RNAi for *SOX2*. SOX2 was also involved in the
740 expression of NOTCH1, MYC, TCF4, Trp53, and RBL1 in *ASCL1*-TF A549 cells. (B) Cell
741 counting assays with SCLC cell lines. The cell growth curve is shown. The suppression of
742 cell proliferation was observed in H69, H889, and SBC1 cells with RNAi against *SOX2*. The
743 analysis was performed in triplicate. Data are shown as the mean ±SD. Asterisks indicate a
744 significant difference. *, $p<0.05$.
745
746 Fig. 4: *SOX2* knockdown in the variant subtype of SCLC cell lines, SBC3 and H69AR
747 cells, using RNAi. *SOX2* mRNA expression significantly decreased, whereas tumor
748 proliferative capacity did not after the knockdown of *SOX2* in SBC3 and H69AR cells. *YAP1*,
749 *TEAD1*, or *VIMENTIN* mRNA expression decreased in *SOX2*-knockout SBC3 and H69AR
750 cells. *ASCL1*, *INSM1*, and *WNT11* mRNA expression did not change in these cell lines. The
751 analysis was performed in triplicate. Data are shown as the mean ±SD. Asterisks indicate a
752 significant difference. *, $p<0.05$.
753

754 Fig. 5: A SCLC precursor lesion in the *Trp53 (-); CCSPrtTA; tetOCre; Rb1 (fl/fl); Hes1*
755 *(fl/fl)* mouse treated with doxycycline for 6 weeks. Serial sections stained with hematoxylin
756 and eosin (HE) and IHC for Ascl1, Sox2, and Insm1. Scale bar = 50 μm.
757
758 Fig. 6: Distinct roles for SOX2 in classical and variant subtypes of SCLC were
759 summarized. ASCL1 and SOX2 cooperatively regulate INSM1 and WNT11 expression and
760 SOX2 affects not only tumor cell proliferation, but also EMT modulation or NE
761 differentiation in the classical subtype. On the other hand, SOX2 affects distinct cell
762 signaling, such as the Hippo pathway, and modulates EMT in the variant subtype. SOX2
763 affects tumor cell survival slightly more in the classical subtype than in the variant subtype
764 of SCLC.
765
766 Supplementary Fig. S1: IHC images of surgically resected non-SCLC tissues for SOX2,
767 and ASCL1. SOX2 was expressed in tumor cell nuclei. Representative images are shown.
768 Scale bar = 200 μm.
769
770 Supplementary Fig. S2: SOX2 affects ASCL1 expression in SCLC cell lines. The
771 suppression of *ASCL1* was observed in the classical subtype of SCLC cell lines, H69, H889,

772 and SBC1, with RNAi for *SOX2* by qRT-PCR. Hippo pathway-related mRNA, *YAP1* and
773 *TEAD1*, did not show significant changes after the knockdown of *SOX2* in these cells. The
774 analysis was performed in triplicate. Data are shown as the mean ±SD. Asterisks indicate a
775 significant difference. *, $p<0.05$.
776
777 Supplementary Fig. S3: *SOX2* knockout in SBC3 and H69AR cells using the
778 CRISPR/Cas9 system. SOX2 protein expression was completely diminished (A), whereas
779 tumor proliferative capacity was not after the knockout of *SOX2* in SBC3 and H69AR cells
780 (B). *YAP1*, *TEAD1,* or *VIMENTIN* mRNA expression decreased in SOX2-knockout SBC3 and
781 H69AR cells (C).
782
783 **The paper explained**
784 PROBLEM
785 Small cell lung cancer (SCLC) is an aggressive neuroendocrine (NE) malignancy with
786 few therapeutic options. *SOX2* is an oncogene, the amplification of which has been reported
787 in human SCLC. However, the role of SOX2 remains unclear and strategies to selectively
788 target SCLC cells have not been established.
789

RESULTS

A chromatin immunoprecipitation sequencing analysis identified distinct putative target genes of SOX2 between the classical and variant subtypes of SCLC cell lines. ASCL1, a lineage-specific transcriptional factor, is involved in NE differentiation and tumorigenesis, and recruited SOX2 to the lineage-specific gene, *INSM1*, in the classical subtype of SCLC. *SOX2* suppression using RNAi resulted in significant reductions in tumor cell proliferative capacity in the classical subtype. On the other hand, SOX2 binds distinct genes, such as those in the Hippo signaling pathway, and the knockdown of *SOX2* was insufficient to inhibit tumor cell growth in the variant subtype of SCLC. SOX2 appears to potently modulate epithelial-to-mesenchymal transition via the Wnt or Hippo signaling pathways and affect tumor cell invasive capacity in each cell in a context-dependent manner.

IMPACT

The present results provide insights into the functional underpinnings of small cell lung carcinogenesis and promote our understanding of SCLC phenotypic changes. The functional discrepancy in SOX2 between the classical and variant subtypes of SCLC may have an impact on appropriate therapeutic approaches and suggests that the ASCL1-SOX2 axis is a promising therapeutic target or biomarker to identify SCLC patients that may

808 benefit from a SOX2-directed therapeutic approach in future clinical trials.

Figure 1

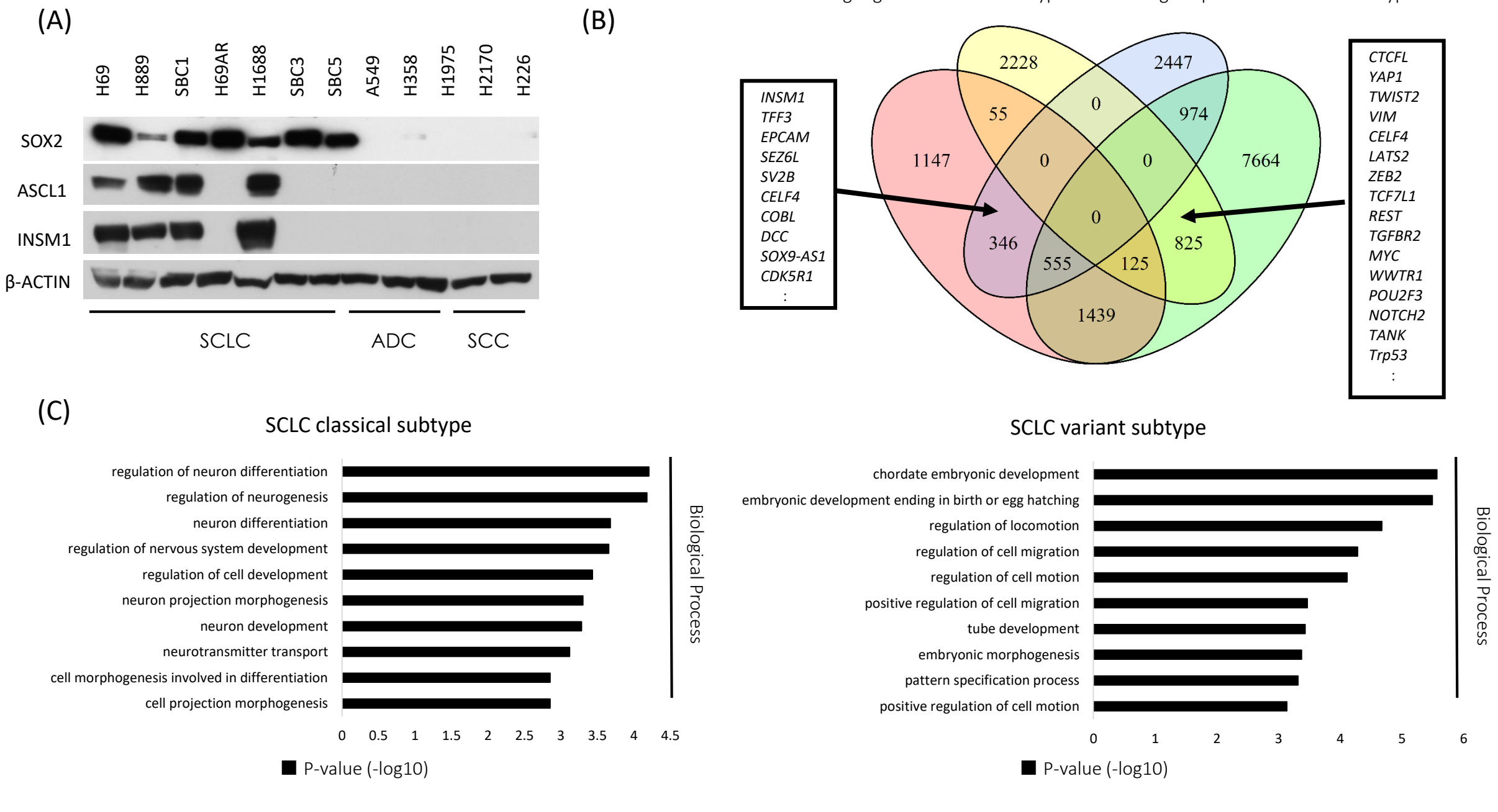
(A)
H69
H889
SBC1
H69AR
H1688
SBC3
SBC5
A549
H358
H1975
H2170
H226
SOX2
ASCL1
INSM1
β-ACTIN
SCLC
ADC
SCC
(B)
SOX2 target genes in classical subtype
SOX2 target genes in variant subtype
high expression in classical subtype
high expression in variant subtype
INSM1
TFF3
EPCAM
SEZ6L
SV2B
CELF4
COBL
DCC
SOX9-AS1
CDK5R1
:
2228
2447
55
0
974
1147
0
0
7664
0
346
555
125
825
1439
CTCFL
YAP1
TWIST2
VIM
CELF4
LATS2
ZEB2
TCF7L1
REST
TGFBR2
MYC
WWTR1
POU2F3
NOTCH2
TANK
Trp53
:
(C)
SCLC classical subtype
regulation of neuron differentiation
regulation of neurogenesis
neuron differentiation
regulation of nervous system development
regulation of cell development
neuron projection morphogenesis
neuron development
neurotransmitter transport
cell morphogenesis involved in differentiation
cell projection morphogenesis
0
0.5
1
1.5
2
2.5
3
3.5
4
4.5
Biological Process
P-value (-log10)
SCLC variant subtype
chordate embryonic development
embryonic development ending in birth or egg hatching
regulation of locomotion
regulation of cell migration
regulation of cell motion
positive regulation of cell migration
tube development
embryonic morphogenesis
pattern specification process
positive regulation of cell motion
0
1
2
3
4
5
6
Biological Process
P-value (-log10)

Figure 2

(A)

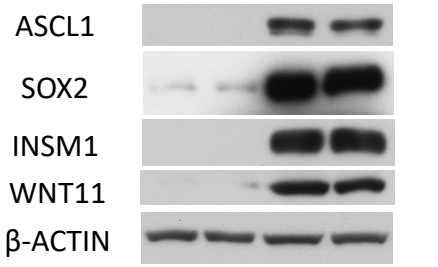

(B)

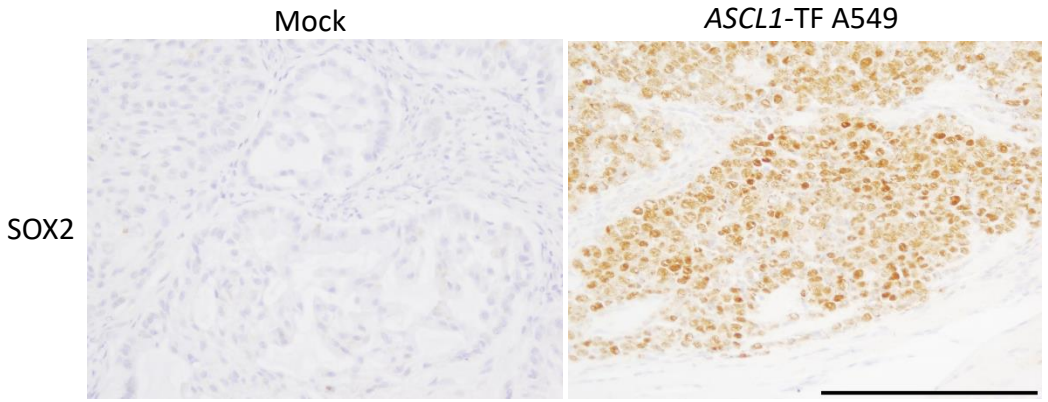

(C)

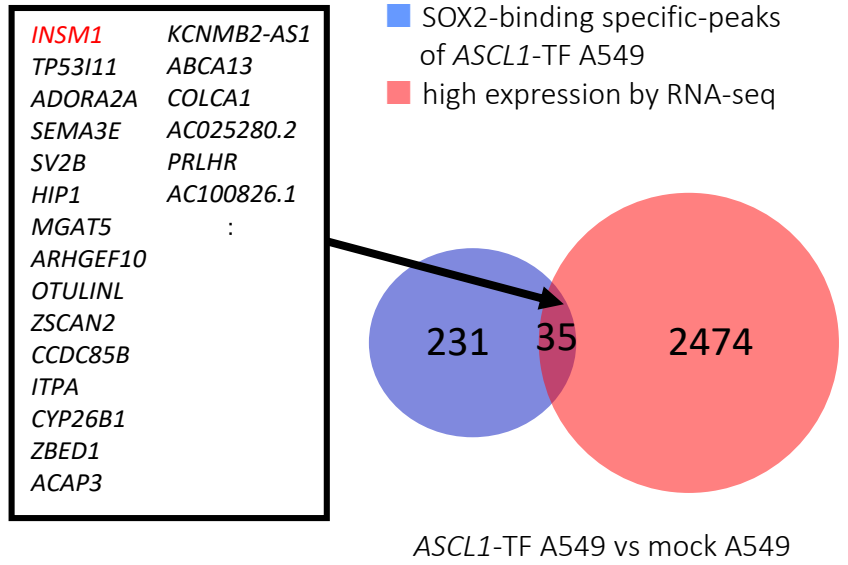

(D)

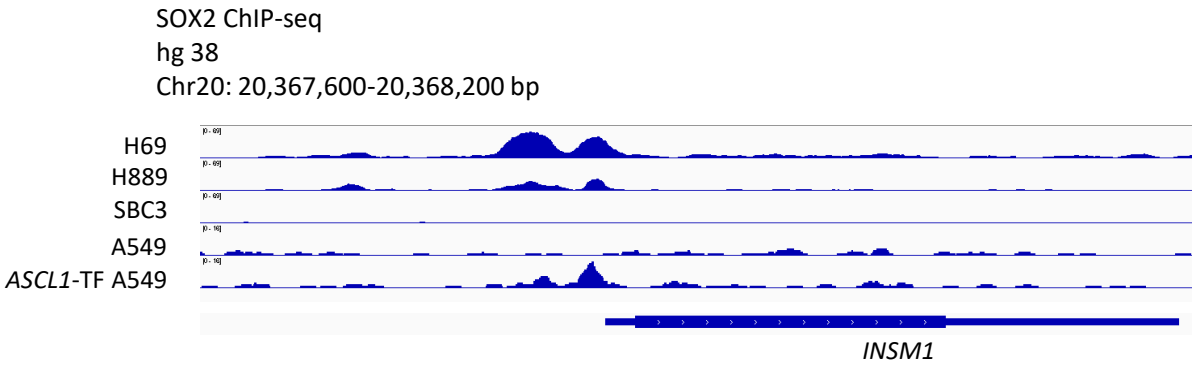

(E)

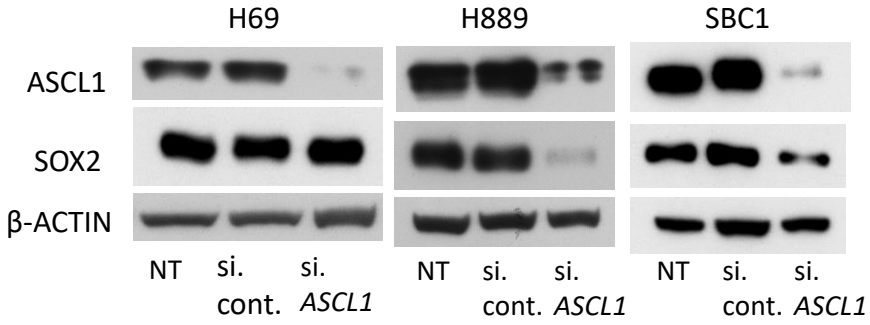

Figure 2

(F)

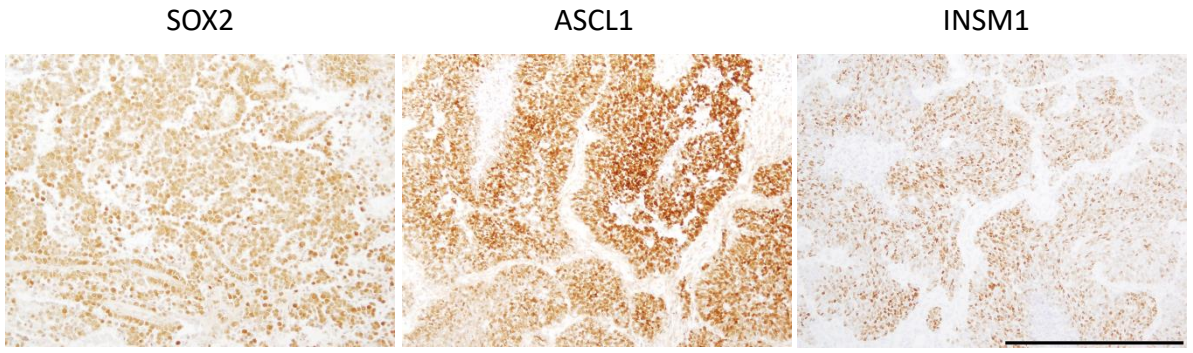

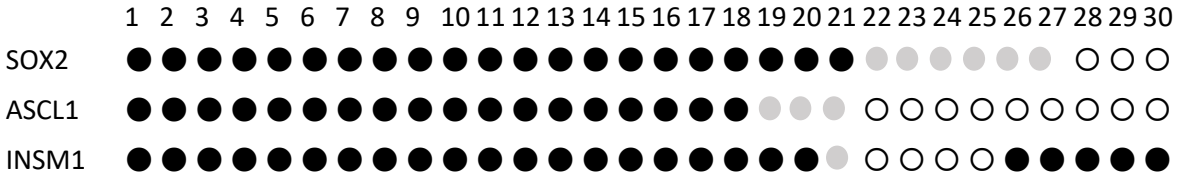

○; score 0, negative ●; score1, weak positive ●; score 2, positive

(G)

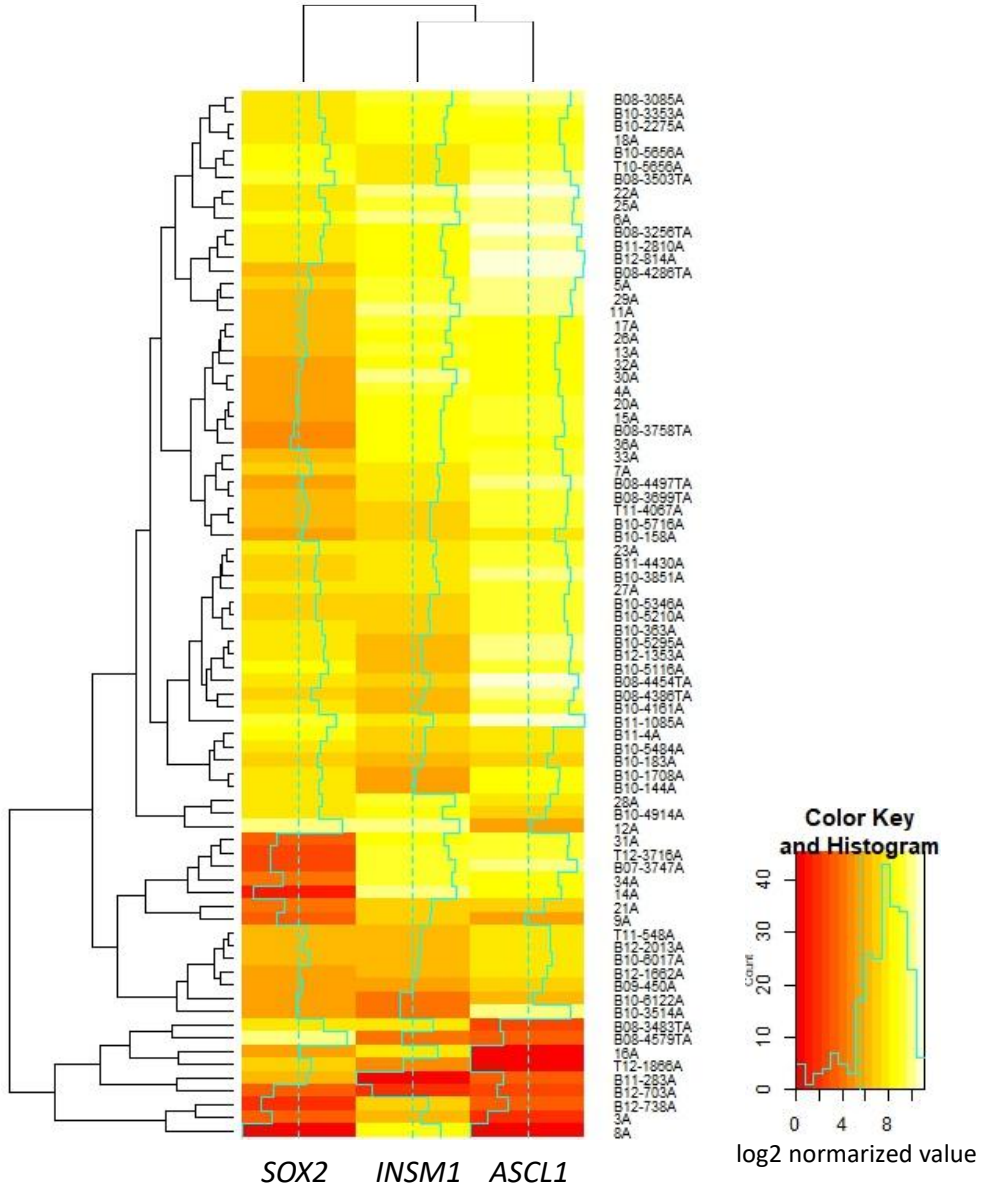

Figure 3

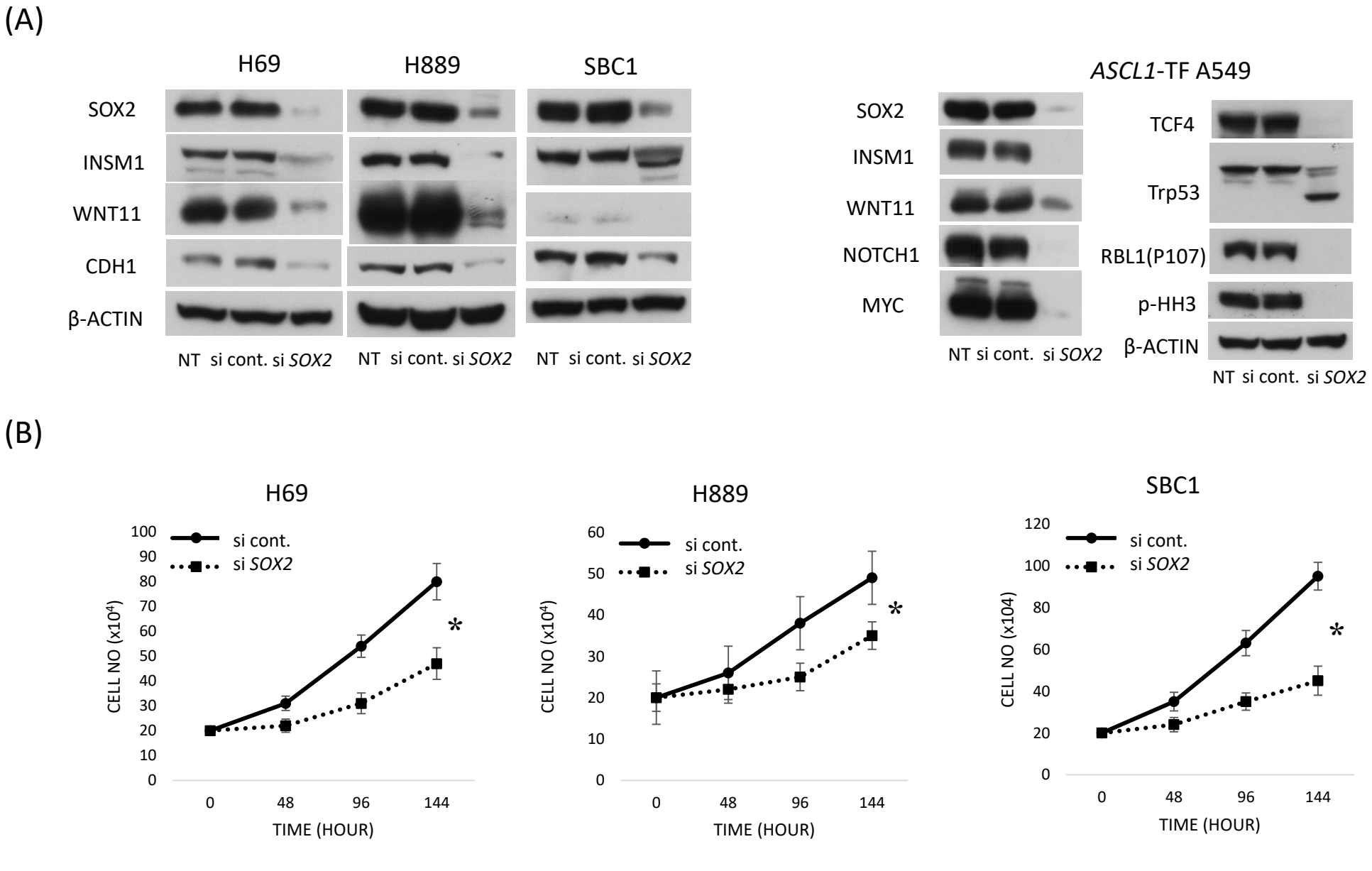
(A)
H69
H889
SBC1
SOX2
INSM1
WNT11
CDH1
β-ACTIN
NT si cont. si SOX2
NT si cont. si SOX2
NT si cont. si SOX2
ASCL1-TF A549
SOX2
INSM1
WNT11
NOTCH1
MYC
NT si cont. si SOX2
TCF4
Trp53
RBL1(P107)
p-HH3
β-ACTIN
NT si cont. si SOX2
(B)
H69
si cont.
si SOX2
CELL NO (x10⁴)
TIME (HOUR)
H889
si cont.
si SOX2
CELL NO (x10⁴)
TIME (HOUR)
SBC1
si cont.
si SOX2
CELL NO (x104)
TIME (HOUR)

Figure 4

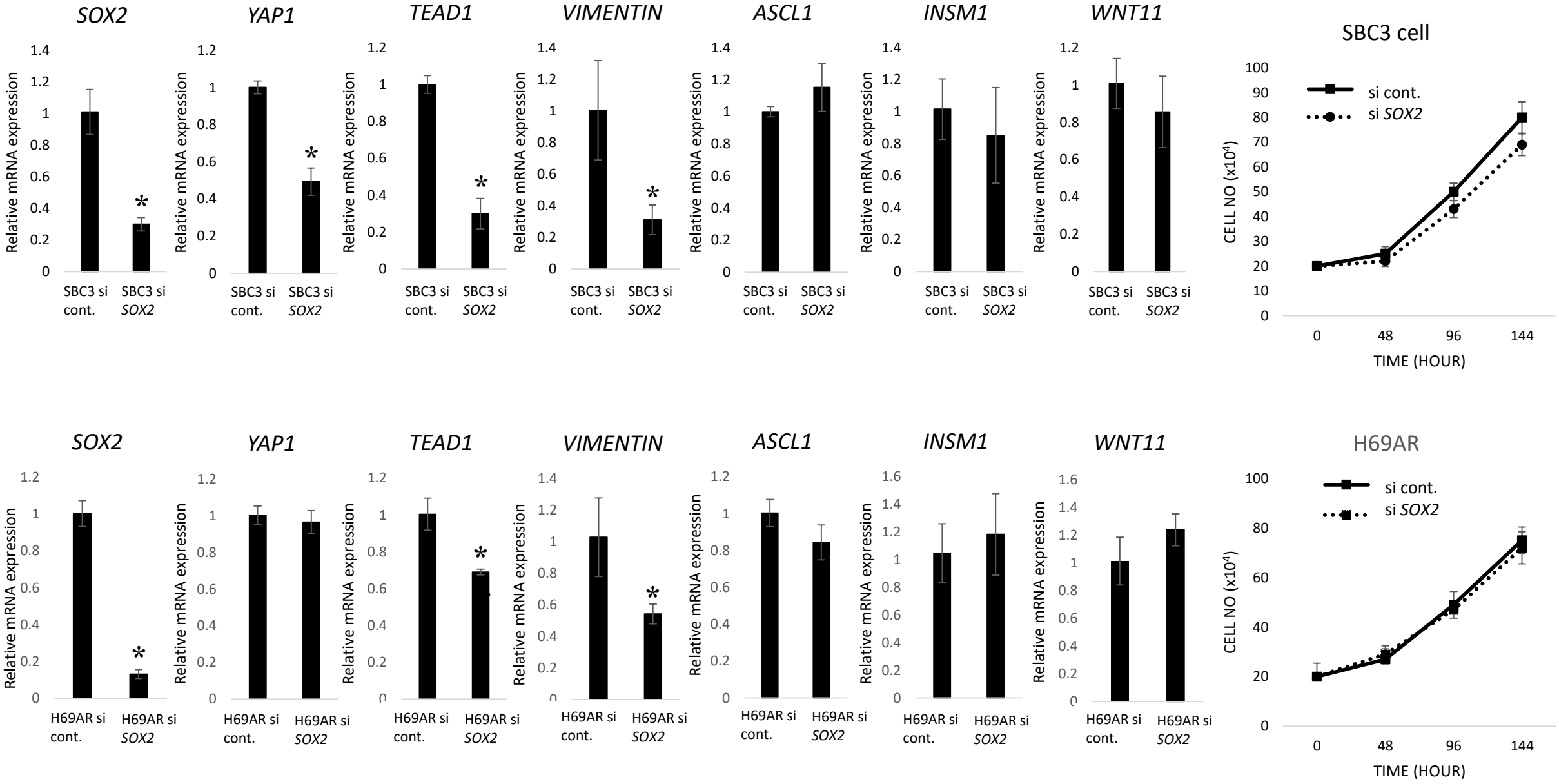
SOX2
YAP1
TEAD1
VIMENTIN
ASCL1
INSM1
WNT11
Relative mRNA expression
SBC3 si cont.
SBC3 si SOX2
SBC3 cell
si cont.
si SOX2
CELL NO (x10⁴)
TIME (HOUR)
H69AR
H69AR si cont.
H69AR si SOX2

Figure 5

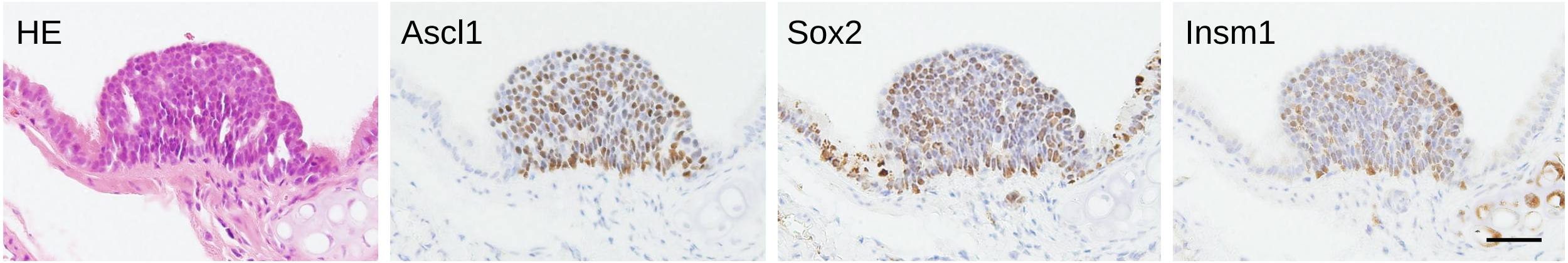

Figure 6

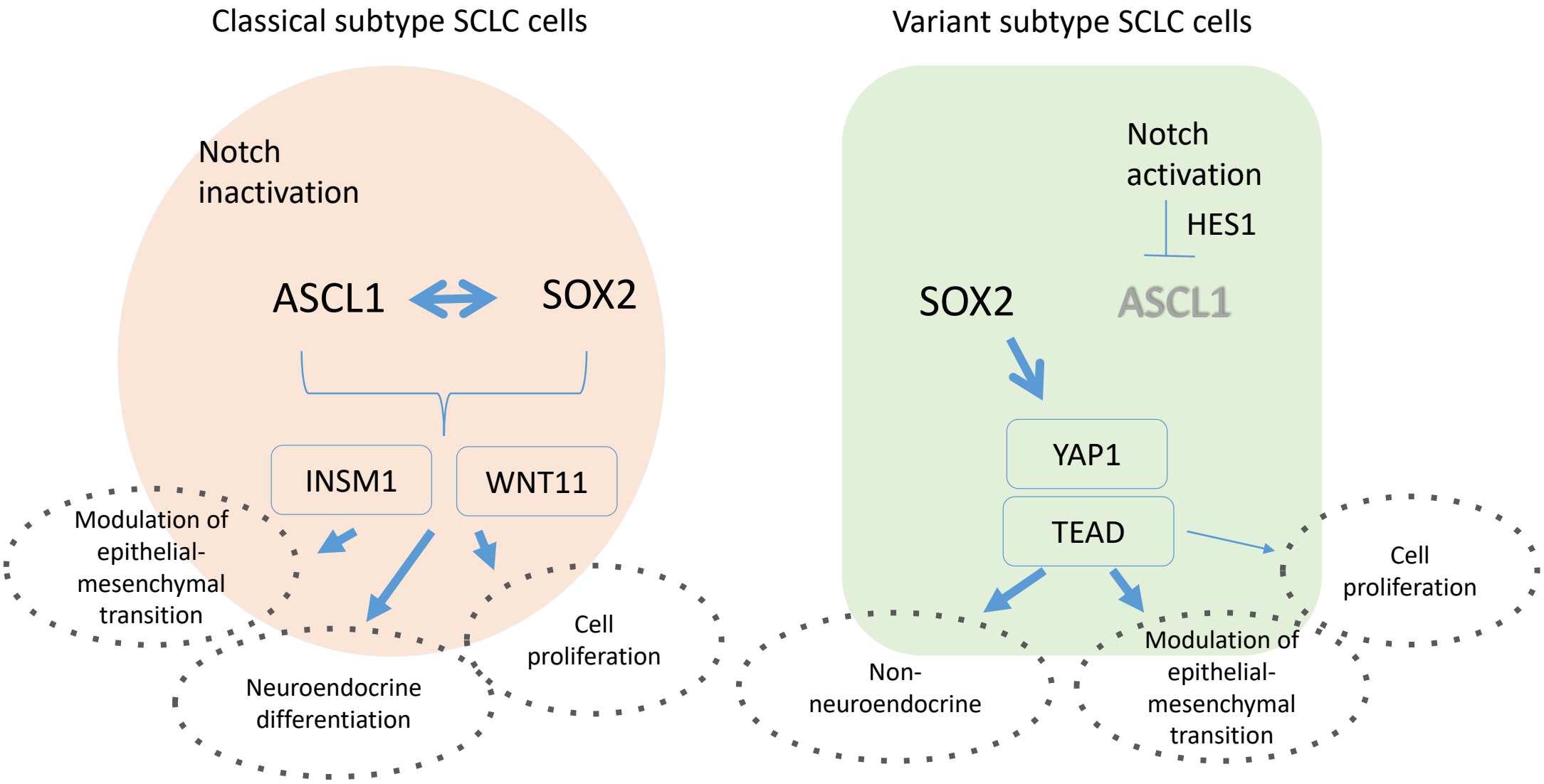
Classical subtype SCLC cells
Notch inactivation
ASCL1
SOX2
INSM1
WNT11
Modulation of epithelial-mesenchymal transition
Neuroendocrine differentiation
Cell proliferation
Variant subtype SCLC cells
Notch activation
HES1
SOX2
ASCL1
YAP1
TEAD
Non-neuroendocrine
Modulation of epithelial-mesenchymal transition
Cell proliferation

Supplementary Figure S1

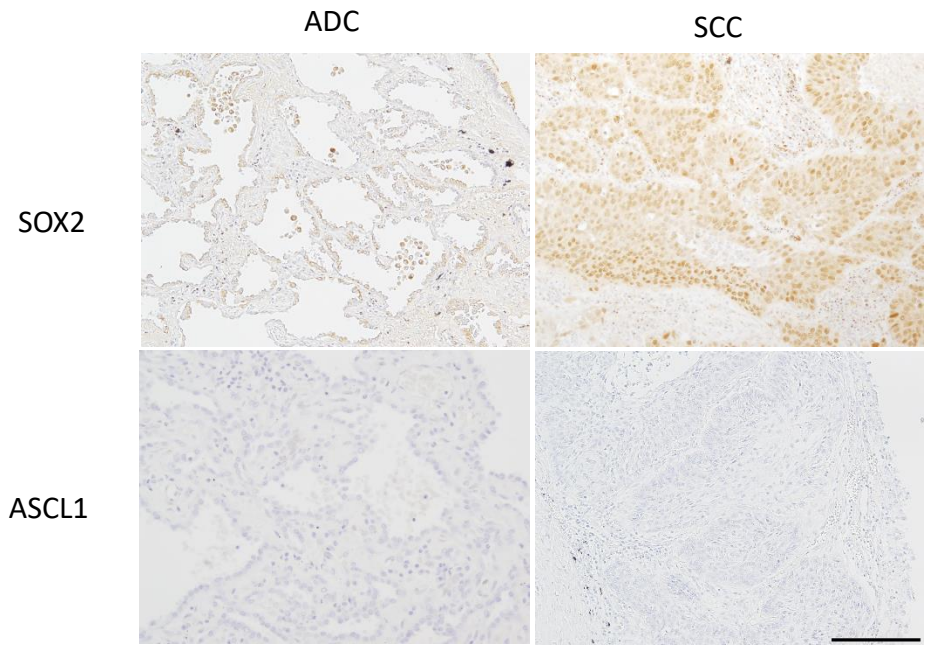

Supplementary Figure S2

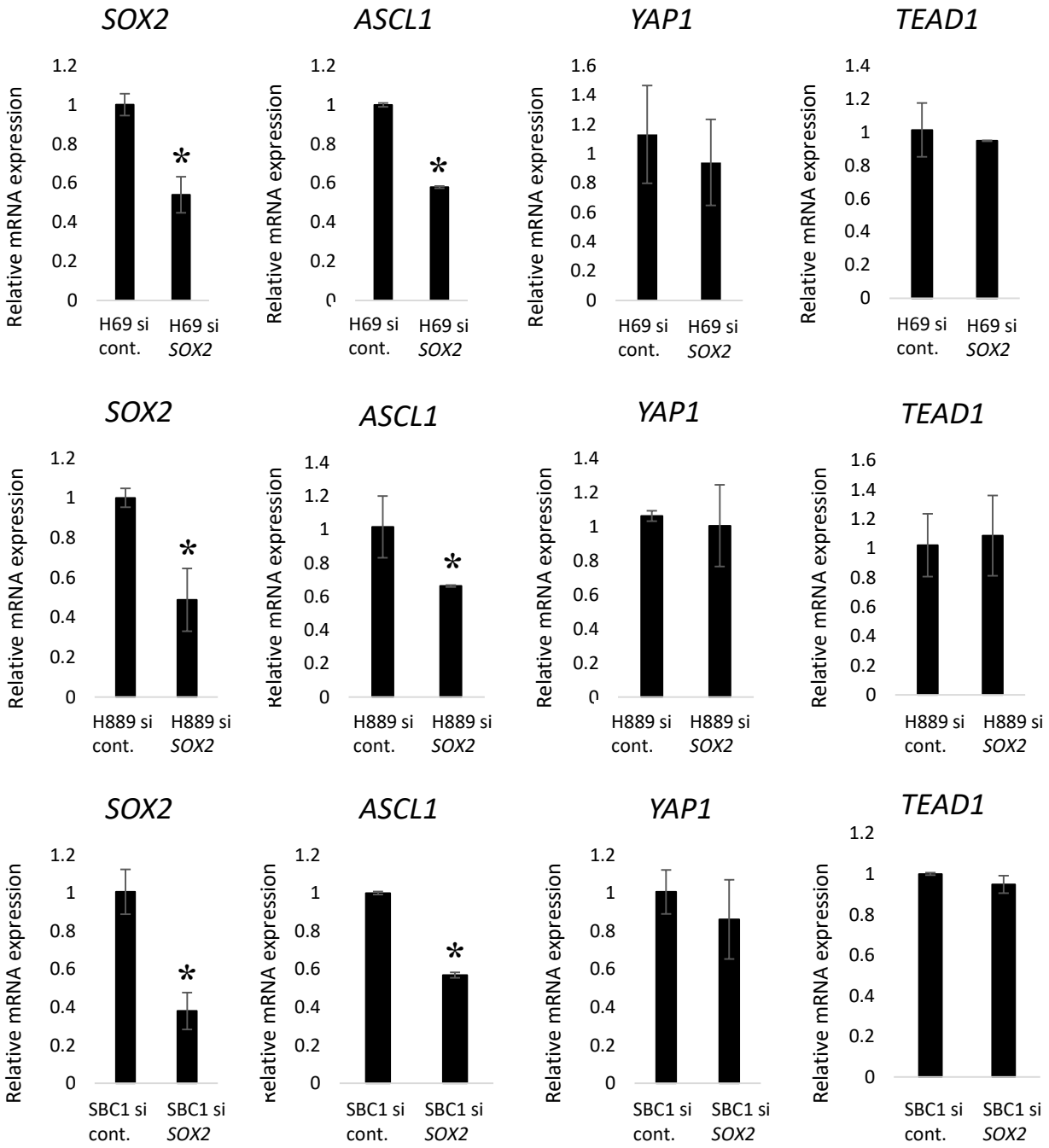

Supplementary Figure S3

(A)

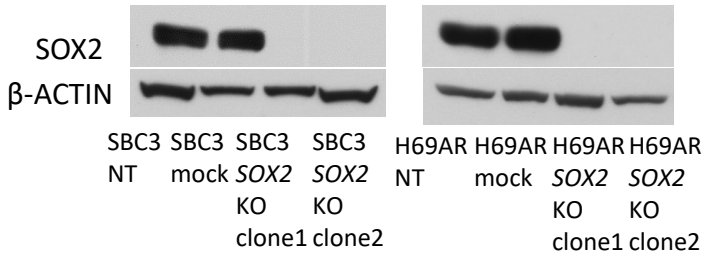

(B)

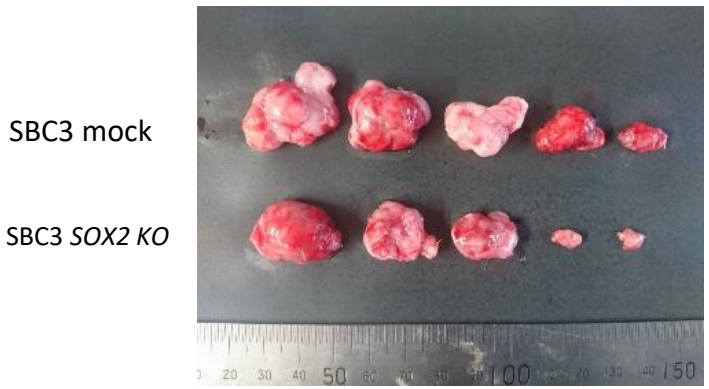

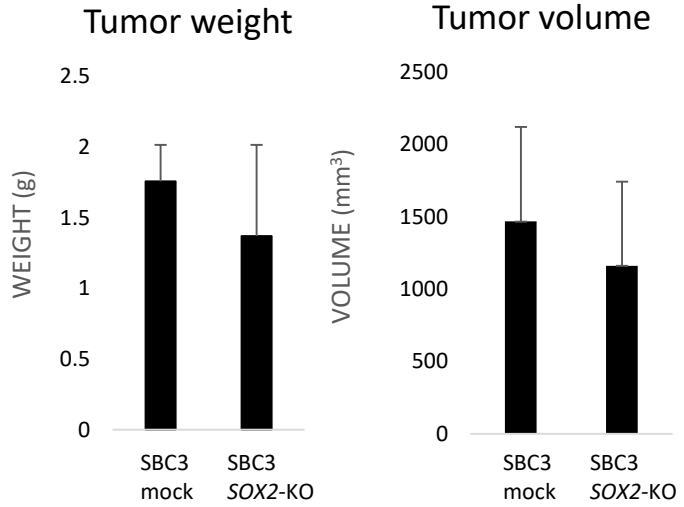

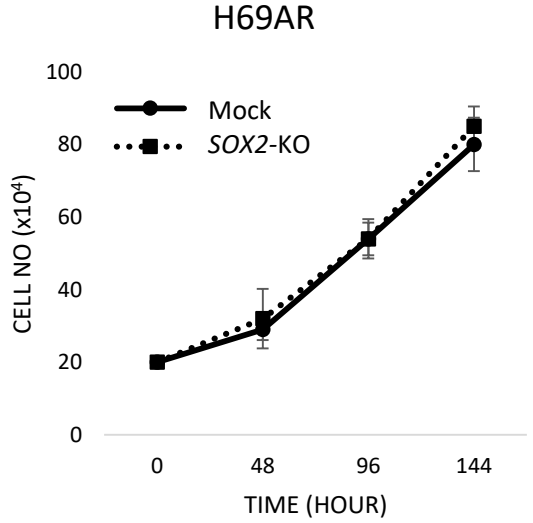

(C)

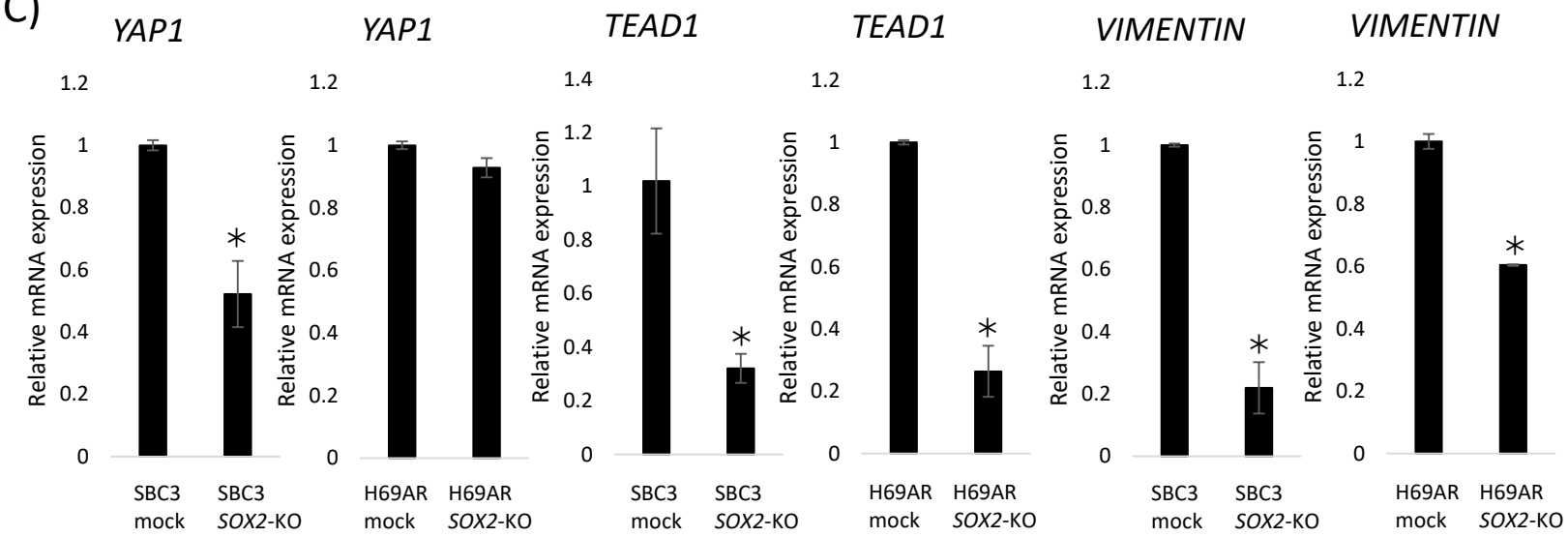

Table 1 Result of Immunohistochemical Staining of Human Lung cancer

	SCLC			ADC
	SOX2	ASCL1	INSM1	SOX2
score				
0, negative	3/30 （10.0%）	9/30 （30.0%）	4/30 (13.3%)	6/20 （30.02%）
1, weak positive	6/30 （20.0%）	3/30 （10.0%）	1/30 (3.3%)	7/20 （30.0%）
2, positive	21/30 （70.0%）	18/30 （60.0%）	25/30 (83.3%)	7/20 （35.0%）

SCLC tissues highly express SOX2, ASCL1, and INSM1. Immunohistochemical staining for SC
specimens that had been surgically resected. Immunohistochemical staining for SOX2 and
specimens. SCLC, small cell lung carcinoma; ADC, adenocarcinoma; SCC, squamous cell car

	SCC	
ASCL1	SOX2	ASCL1
17/20（85.0%）	4/20（20.0%）	16/20（80.0%）
3/20（15.0%）	5/17（25.0%）	4/20（20.0%）
0/20（0%）	11/20（55.0%）	0/20（0%）

)X2, ASCL1, and INSM1 was performed in 30 SCLC
ASCL1 was also performed in 20 ADC and 20 SCC
cinoma

Table 2 Antibodies used for IHC and WB analysis

Primary antibody	Manufacturer（location）	WB	IHC
Sox2 (AB5603)	Millipore (Billerica, MA)	1:1000	1:100
Sox2 (E-4)	Santa Cruz Biotechnology		1:1000
ASH1 (AB15582)	Millipore (Billerica, MA)		1:100
MASH1 (ab213151)	abcam (Cambridge, UK)		1:1000
Ascl1 (556604)	BD Biosciences (San Jose, CA)	1:500	
Wnt11 (107-10576)	RayBiotech (Norcross, GA)	1:1000	
Insm1 (C-1)	Santa Cruz Biotechnology	1:5000	
E-cadherin (610181)	BD Biosciences	1:1000	
Notch1 (D1E11)	Cell Signaling	1:1000	
c-Myc (D84C12)	Cell Signaling	1:1000	
TCF4 (D-4)	Santa Cruz Biotechnology	1:1000	
p53 (DO-1)	Santa Cruz Biotechnology	1:1000	
p107 (C-18)	Santa Cruz Biotechnology	1:1000	
p-Histone H3 (Ser10)	Millipore (Billerica, MA)	1:500	
β-actin (A-5441)	Sigma Aldrich (Oakville, ON, Canada)	1:10000	

Manufacturers, quantities, and working dilutions are indicated. Ascl1, achaete-scute complex homolog-like 1; Wnt11, Wnt family member 11; Insm1, insulinoma-associated protein 1; TCF4, transcription factor 4; IHC, immunohistochemistry; WB, Western blot.

Table 3 List of primers used in PCR

Target	Sequence	Product size (bp)
SOX2	F: 5 -AACCCCAAGATGCACAACTC-3′ R: 5 -CGGGGCCGGTATTTATAATC-3′	152
ASCL1	F: 5-CGGCCAACAAGAAGATGAGT-3′ R: 5-GCCATGGAGTTCAAGTCGTT-3′	169
INSM1	F: 5-CAGTGTGCGGAGAGTCGTT-3′ R: 5-ACCTGTCTGTTTTCGGATGG-3′	166
WNT11	F: 5-TGACCTCAAGACCCGATACC-3′ R: 5-GCTTCCGTTGGATGTCTTGT-3′	189
YAP1	F: 5 -GCAGTTGGGAGCTGTTTCTC -3′ R: 5 -GCCATGTTGTTGTCTGATCG -3′	203
TEAD1	F: 5 -TCAGCTTTTCTCGAGCAGCA-3′ R: 5 -CACACAGGCCATGCAGAGTA-3′	555
VIMENTIN	F: 5 -GAGAACTTTGCCGTTGAAGC -3′ R: 5 -TCCAGCAGCTTCCTGTAGGT -3′	170
GAPDH	F: 5 -CAGCCTCAAGATCATCAGCA -3′ R: 5 -TGTGGTCATGAGTCCTTCCA -3′	106

SOX2, SRY-box 2; ASCL1, achaete-scute complex homolog-like 1; INSM1, insulinoma-associated protein 1; WNT11, Wnt family member 11; YAP1, Yes associated protein 1; TEAD1, TEA domain transcription factor 1; GAPDH, glyceraldehyde-3-phosphate dehydrogenase; F, forward; R, reverse.